ELSEVIER

Palaeogeography, Palaeoclimatology, Palaeoecology 187 (2002) 35–60

PALAEO

www.elsevier.com/locate/palaeo

High-stress paleoenvironment during the late Maastrichtian to early Paleocene in Central Egypt

Gerta Keller[a,*], Thierry Adatte[b], Stephen J. Burns[c], Abdel Aziz Tantawy[d]

[a] Department of Geosciences, Princeton University, Princeton, NJ 08540, USA
[b] Geological Institute, University of Neuchâtel, 2007 Neuchâtel, Switzerland
[c] Department of Geosciences, University of Massachusetts, Amherst, MA 01003, USA
[d] Department of Geology, Faculty of Science, South Valley University, Aswan 81528, Egypt

Received 19 September 2001; received in revised form 24 April 2002; accepted 18 July 2002

Abstract

Biostratigraphic, mineralogical, geochemical and isotopic analyses of the Gebel Qreiya section in the Asyut Basin of central Egypt indicate a depositional environment interrupted by periods of erosion due to local tectonic activity exacerbated by eustatic sea-level fluctuations, and by high-stress environmental conditions akin to those normally experienced during the Cretaceous–Tertiary boundary transition. During the late Maastrichtian (66.8–65.4 Ma) this region experienced a breakdown of the biologically mediated surface to bottom gradient of the $^{13}C/^{12}C$ ratio with planktic $\delta^{13}C$ values 0.2–0.8‰ lighter than benthic values. Planktic foraminiferal species diversity was reduced by more than 50%, with faunal assemblages dominated (75–90%) by the opportunistic disaster species *Guembelitria cretacea*, which alternate with abundance of small, low oxygen-tolerant heterohelicids (*Heterohelix navarroensis*, *H. dentata*, *H. globulosa*). This prolonged breakdown in ocean primary productivity occurred during a time of global climate cooling and sea-level regressions (at 66.8 and 65.5 Ma), though clay mineralogy suggests that locally low seasonality warm, wet, tropical and subtropical conditions prevailed. The high detrital influx suggests that the biologically high-stress environment was primarily linked to the existing shallow shelf conditions in southern Egypt, and possibly to local tectonic activity and restricted circulation. A normal carbon isotope gradient was briefly re-established during the short climate warming and rising sea level between 65.4 and 65.2 Ma, a time of increased species diversity, peak abundance of rugoglobigerinids and common heterohelicids. During the last 200 000 years of the Maastrichtian, increased precipitation and terrestrial runoff (increased phyllosilicates and kaolinite) and increasing total organic carbon values are associated with *Heterohelix*-dominated planktic foraminiferal assemblages. The K/T boundary is marked by a red clay layer and Ir anomaly of 5.4 ppb. During the early Danian, planktic foraminiferal populations and stable isotope data indicate that similarly fluctuating high-stress conditions prevailed in central Egypt as elsewhere in the marginal eastern Tethys.

Keywords: high-stress late Maastrichtian paleoenvironment

1. Introduction

The stratigraphic and lithologic records of the Cretaceous–Tertiary (K/T) transition in Egypt are variable depending on the depositional environ-

* Corresponding author.
E-mail address: gkeller@princeton.edu (G. Keller).

PII: S0031-0182(02)00504-7

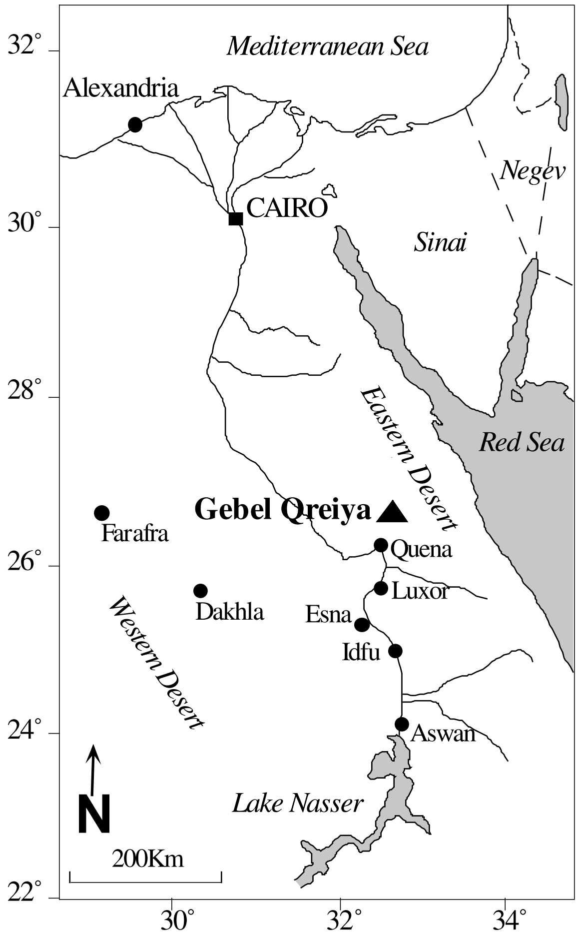

Fig. 1. Location of the Gebel Qreiya section, Central Egypt.

ment. In the Western Desert sediment deposition occurred in a shallow marginal sea which deepened to the northwest (Farafra Oasis, Fig. 1). In this region the K/T boundary is missing from Dakhla to Farafra primarily due to erosion as a result of local tectonic activity and a sea-level regression (Issawi, 1972; Garrison et al., 1979; Barthel and Herrmann-Degen, 1981; Hendriks et al., 1987; Ganz et al., 1990a,b; Hermina, 1990; Glenn, 1990; Schnack and Luger, 1998; Tantawy et al., 2001). In the Eastern Desert, the Sinai and Negev, sediment deposition occurred in a deeper middle to outer shelf environment where sediment deposition was primarily interrupted by erosion due to global sea-level fluctuations (Sestini, 1984; Hendriks et al., 1987; Luger, 1988; Jenkyns, 1990; Keller and Benjamini, 1991; Strougo et al., 1992; Kassab and Keheila, 1994; Luger et al., 1989). As a result, the K/T transition is largely discontinuous in these regions also, though hiatuses tend to encompass much smaller intervals than in the Western Desert.

The Gebel Qreiya section is among the most complete upper Maastrichtian to Danian sequences in the Eastern Desert and among the very few localities where the planktic foraminiferal zone *Parvularugogloberina eugubina* and calcareous nannofossil zone NP1 are present (e.g. East Qena region, Luger, 1988; Luger et al., 1989; Duwi region, Tantawy, 1998; St. Paul, South Galala, Strougo et al., 1992; Faris, 1995, 1997; Keller, 2002; Tantawy, in press). Gebel Qreiya was located on the stable shelf of the Asyut Basin (Fig. 1, Said, 1962) at about middle to outer shelf depths. This region was subject to sea-level fluctuations throughout the late Cretaceous and early Tertiary (Hendriks et al., 1987; Luger and Groeschke, 1989). During the early Maastrichtian sea-level transgression, open marine conditions were established throughout central Egypt and to the south. During subsequent sea-level regressions, erosion was widespread and extensive in the marginal seas to the south and west coupled with local tectonic activity in the Western Desert (Hendriks et al., 1987; Schnack and Luger, 1998; Tantawy et al., 2001). But in the Eastern Desert, erosion was generally more limited. In this region sediment deposition during the late Cretaceous and early Paleocene was primarily controlled by large-scale rejuvenation of the pre-existing fault system (Hendriks et al., 1987), with major erosion linked to active uplift during the late Campanian to early Maastrichtian. During the late Maastrichtian to early Paleocene sediment deposition was controlled primarily by sea-level fluctuations, as suggested also by less diverse lithologies (Hendriks and Luger, 1987).

This report focuses on the Gebel Qreiya section as reference point to evaluate the age and depositional environment of central Egypt during the late Maastrichtian and early Paleocene. Age control is based on quantitative analyses of calcareous nannofossils (Tantawy, in press) and planktic foraminifera (Keller, 2002). Paleoenvironmental and paleoecological conditions are evaluated based on an interdisciplinary approach that integrates microfossil biostratigraphies and paleoecology, stable isotope analysis of monospecific planktic and benthic foraminifera, sedimentology, geochemistry and mineralogy. The primary objectives of this study include: (a) high resolution age control, including the recognition of hiatuses and their evaluation within the context of local tectonic activity and global sea-level fluctuations, and (b) environmental interpretation based on faunal and floral changes, stable isotopes, geochemistry and mineralogy.

2. Location and lithology

The Gebel Qreiya section is located at the southern end of Wadi Qena, about 50 km northeast of Qena City and 18 km north of Km53 of the Qena-Safaga road (Lat. 26°21′N Long. 33°01′E, Fig. 1). The Cretaceous–Tertiary boundary lies within the Dakhla Formation, which is widely distributed in central and southern Egypt, though with variable lithologies (e.g. Said, 1962; Abdel Razik, 1969, 1972; Faris, 1984, 1997; Soliman et al., 1986). The upper Maastrichtian sediments consist of monotonous gray shales containing numerous *Pecten farafrensis* casts which decrease upsection (Figs. 2 and 3). About 1.8 m below the K/T boundary shales grade into marly shales devoid of macrofossils (Fig. 3). About 10 cm below the K/T boundary is a pronounced undulating erosional surface with burrows. The 10 cm interval consists of bioturbated marly shale containing macrofossils (*Pecten farafrensis*, Fig. 3). The top of this 10 cm interval is marked by another erosional surface that underlies a 1 cm-thick red clay layer that marks the K/T boundary and contains an Ir anomaly of 5.4 ppb. Above the red layer the basal Danian sediments consist of fissile dark gray marly shales (50 cm), followed by gray shale (∼2 m, Fig. 3).

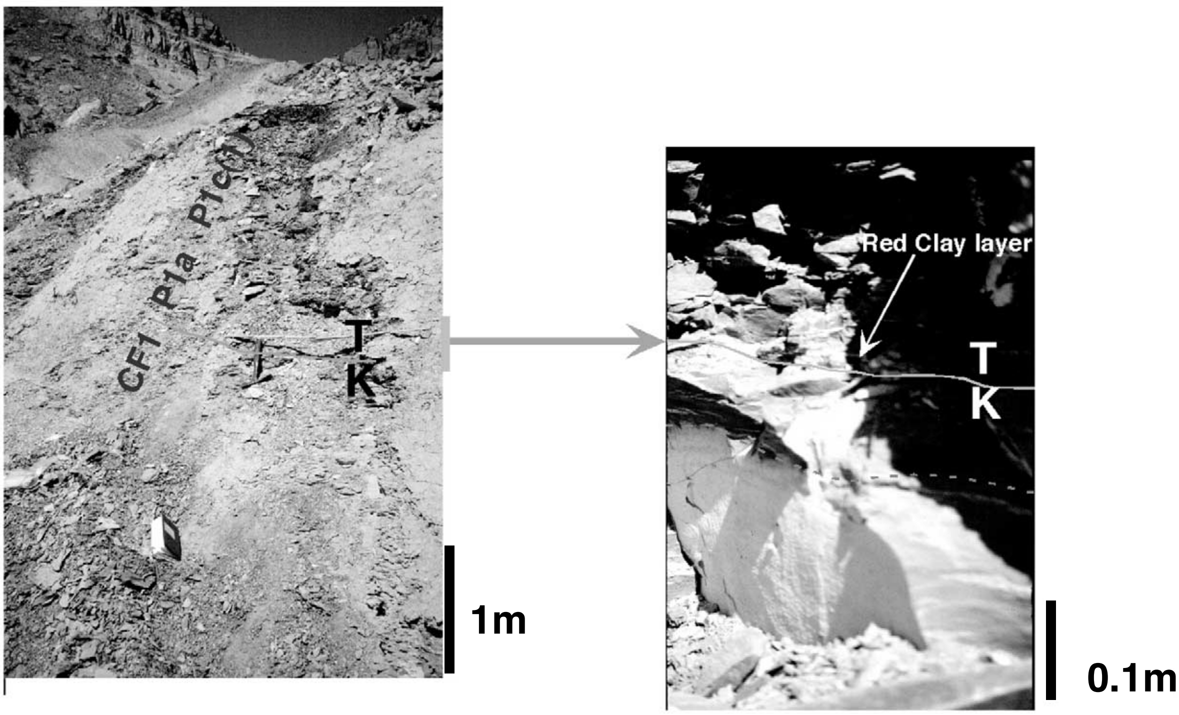

Fig. 2. Photographs of the Gebel Qreiya outcrop showing the Cretaceous–Tertiary boundary marked by a thin red clay layer, zone Pla, P1c(1) and the late Maastrichtian zone CF1.

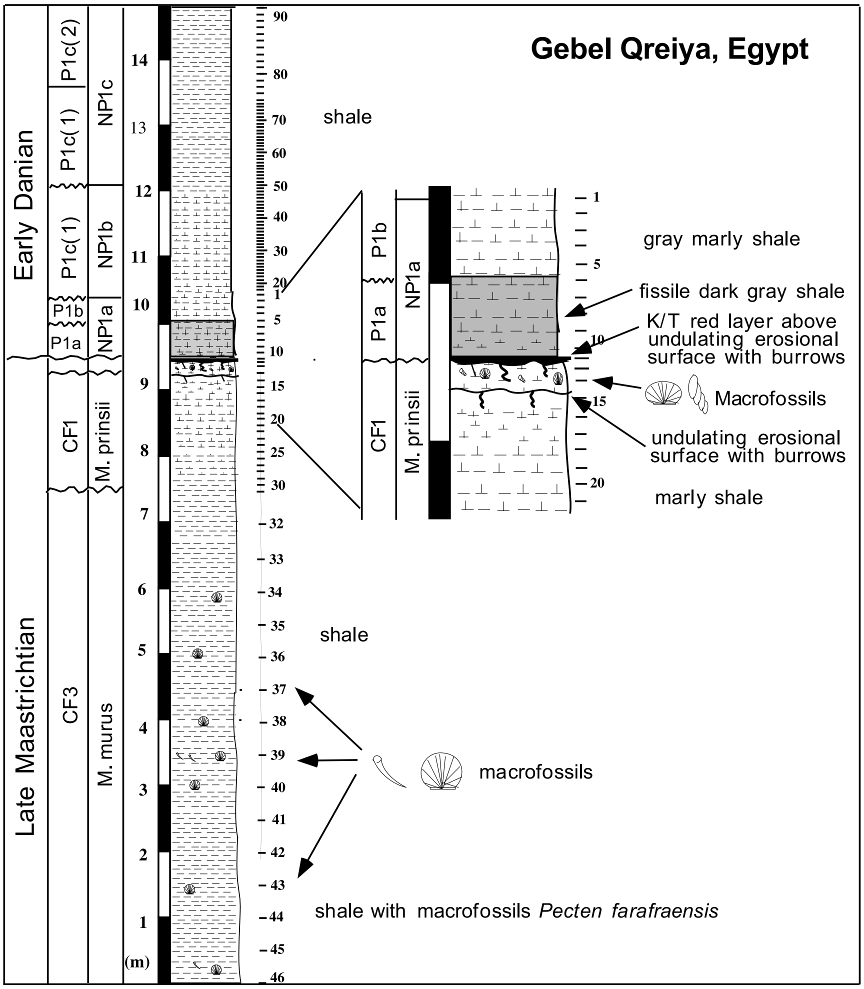

Fig. 3. Lithology of the Gebel Qreiya section. Hiatuses and undulating erosion surfaces are marked by wavy lines. Note that the K/T red layer that contains the Ir anomaly consists of a 1 cm-thick red clay that overlies a hiatus marked by an undulating erosional surface with truncated burrows.

3. Methods

In the field the section was measured and examined for lithological changes, macrofossils, trace fossils, bioturbation, erosion surfaces and hardgrounds. Samples were collected for microfossils, geochemical and mineralogical analyses at 50 cm intervals, except for the Cretaceous–Tertiary transition, which was sampled at 5–10 cm intervals. For foraminiferal study samples were processed following the standard method of Keller et al. (1995). Planktic foraminifera are generally abundant and well preserved, though in some intervals increased carbonate dissolution was observed. The strongest dissolution is observed in the Danian zone Plc(2) (samples 72–86) where nearly all planktic foraminifera are dissolved. Dissolution effects in the lower part of zone Plc(l) are apparent by the abundance of broken specimens and thin test walls. No dissolution effects are apparent in the late Maastrichtian sediments, though low abundance of specimens and the presence of pyrite in samples 34–39 suggest low oxygen conditions. Planktic foraminiferal species were analyzed based on the >63 μm size fraction and about 300 individuals per sample. However, since this size fraction favors small species, the >150 μm size fraction was also analyzed for the Maastrichtian (there are no Danian species in the >150 μm size fraction). Species identification follows standard taxonomic concepts (Robaszynski et al., 1983-1984; Caron, 1985; Nederbragt, 1991, 1998; Olsson et al., 1999). Key index species are illustrated in Plates I and II.

Calcareous nannofossils were processed by standard smear slide preparation from raw sediment samples as described by Perch-Nielsen (1981a,b, 1985). Smear slides were examined using a light photomicroscope with 1000–2000× magnification. Calcareous nannofossils are generally abundant and well preserved. Quantitative analysis was based on smear slides of unprocessed sedimentary samples to prevent loss of smaller-sized specimens. Relative species abundances were determined based on about 300 specimens along a random traverse with a light microscope at a magnification of about 1250× and rare species were searched in additional transects as described in Jiang and Gartner (1986). Data are discussed in Tantawy (in press).

Stable isotope analyses were done separately on left and right coiling specimens of the benthic foraminifer *Cibicidoides pseudoacutus* at Gebel Qreiya and El Kef, Tunisia, in order to test the hypothesis that a change in coiling direction reflects climatic changes as proposed by Coccioni and Galeotti (1998) and Galeotti and Coccioni, 2002). For the late Maastrichtian the surface-dwelling planktic foraminifer *Rugoglobigerina rugosa* was analyzed. Analyses were conducted at the laboratory of the University of Bern, Switzerland, using a VG Prism II ratio mass spectrometer equipped with a common acid bath. The results are reported relative to the VPDB standard reference material with a standard error of 0.1‰ for oxygen and 0.05‰ for carbon.

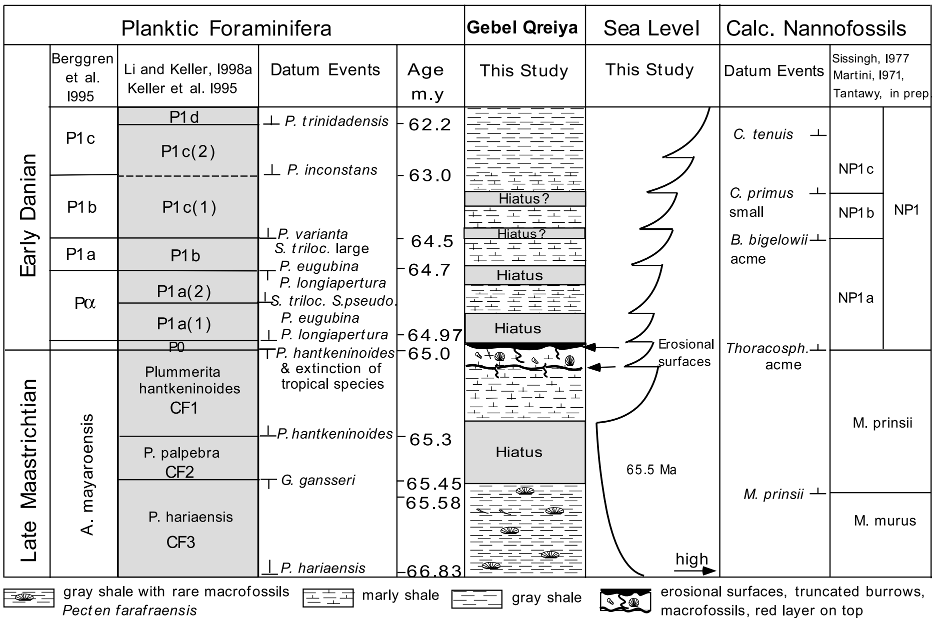

Fig. 4. Planktic foraminiferal biozonation and datum events used in this study are from Keller et al. (1995) and Li and Keller (1998a); the Berggren et al. (1995) biozonation is given for comparison. Calcareous nannofossil biozonation is based on Sissingh (1977), Martini (1971) and Tantawy, in press). Lithological changes, macrofossils, undulating erosional surfaces and hiatuses in the Gebel Qreiya section indicate an interrupted sediment record probably as a result of sea-level fluctuations. Age estimates for late Maastrichtian biozones are based on foraminiferal datum events of DSDP Site 525 tied to the paleomagnetic stratigraphy of the same core, and biostratigraphic correlation with El Kef, Tunisia (Li and Keller, 1998c; Li et al., 1999). Age estimates for Danian biozones are from Berggren et al. (1995). Ages for these Maastrichtian and Danian datum events and biozones are broadly valid for the eastern Tethys region, including Egypt.

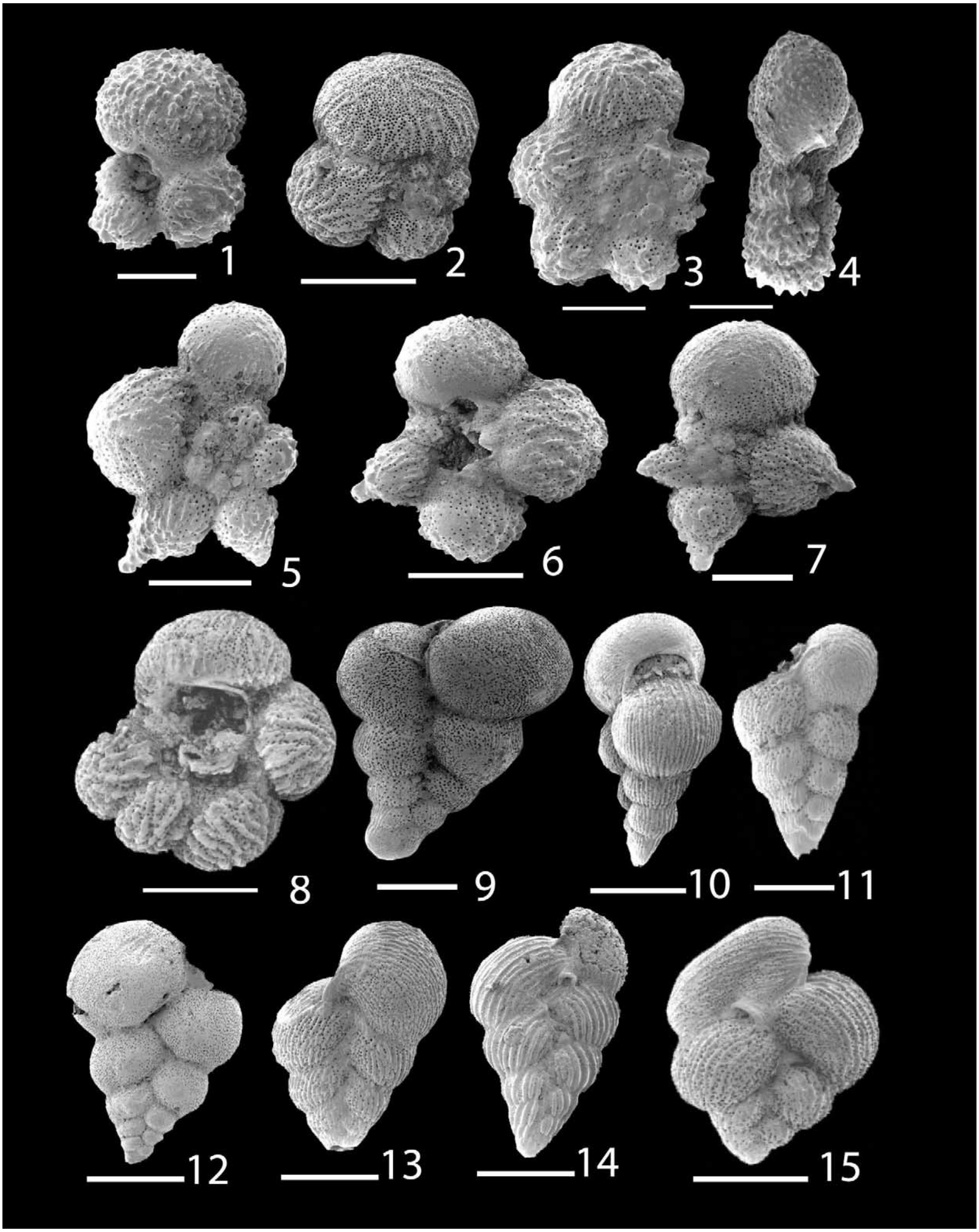

Plate I.

Whole rock and clay mineral compositions were analyzed at the Geological Institute of the University of Neuchâtel, Switzerland, using a Scintag XRD 2000 Diffractometer based on methods described by Kübler (1983, 1987) and Adatte et al. (1996). Total organic carbon (TOC) analysis was performed with a Rock Eval 6 pyrolyser on powdered bulk samples, based on the analytical methods of Espitalié et al. (1986a–c).

4. Biostratigraphy

Planktic foraminifera and calcareous nannofossils of the Gebel Qreiya section are relatively well preserved and abundant and provide excellent biostratigraphic control as discussed in Keller (2002) and Tantawy (in press) and only a brief summary is provided here (Fig. 4). The Qreiya section analyzed spans from the late Maastrichtian planktic foraminiferal zone CF3 and calcareous nannofossil *Micula murus* zone to the early Danian zones Plc and NP2, respectively. All nannofossil zones and all planktic foraminiferal zones, except the short interval of CF2, are at least partially present. However, several hiatuses in this section reflect erosion at times of low sea levels and/or tectonic activity (Fig. 4). The basal 7.5 m of the section spans zone CF3 and the *M. murus* zone (Figs. 5 and 6). The presence of *M. murus* in this interval suggests that the lower part of zone CF3, which corresponds to the upper *Lithraphidites quadratus* zone, was not recovered. Zone CF2 is missing (juxtaposition of index species *Gansserina gansseri* and *Plummerita hantkeninoides*, Plate I, Figs. 5–7), and marks a hiatus correlative with a sea-level lowstand at 65.5 Ma. Zone CF1 (range of *P. hantkeninoides*) and *M. prinsii* zone mark the uppermost 1.8 m of the Maastrichtian. A burrowed erosional surface marks another short hiatus and probably lower sea level about 10 cm below the K/T boundary clay layer (Figs. 3 and 4). The 10 cm thick interval bounded by these two hiatuses contains macrofossils, including bivalves and gastropods that may have been transported from shallower environments to the south (Luger, 1988; Luger et al., 1989).

Throughout Egypt, including the Sinai and the Negev, the K/T boundary interval is generally condensed, often highly bioturbated and frequently marked by erosion surfaces. As a result, the characteristic K/T boundary clay layer and basal red layer that mark zone P0 and contain the Ir anomaly are generally absent or unrecognizable due to erosion and sediment mixing by bioturbation (Keller and Benjamini, 1991; Shahin, 1992; Faris, 1997; Luger et al., 1998; Tantawy et al., 2001). However, at Gebel Qreiya the K/T boundary is marked by a 1 cm-thick red clay layer and thin layer of diagenetic gypsum, similar to that at the stratotype section at El Kef and other complete K/T transitions. An Ir anomaly of 5.4 ppb was identified in this red clay layer (sample 11.5) and marks the first reported occurrence of this anomaly in Egypt. The red layer is devoid of microfossils and overlies an undulating burrowed erosional surface that indicates another short hiatus.

Above the K/T red layer, the simultaneous first

Plate I. Scale bar = 200 μm. All specimens from the latest Maastrichtian zone CF1 (*Plummerita hantkeninoides*) at Qreiya, Egypt.

1, 2. *Rugoglobigerina macrocephala*
3, 4. *R. scotti*
5–7. *Plummerita hantkeninoides*
8. *R. rugosa*
9. *Heterohelix navarroensis*
10. *H. globulosa*
11. *H. dentata*
12. *H. planata*
13. *Laeterohelix labellosa*
14. *Pseudoguembelina costulata*
15. *P. palpebra*

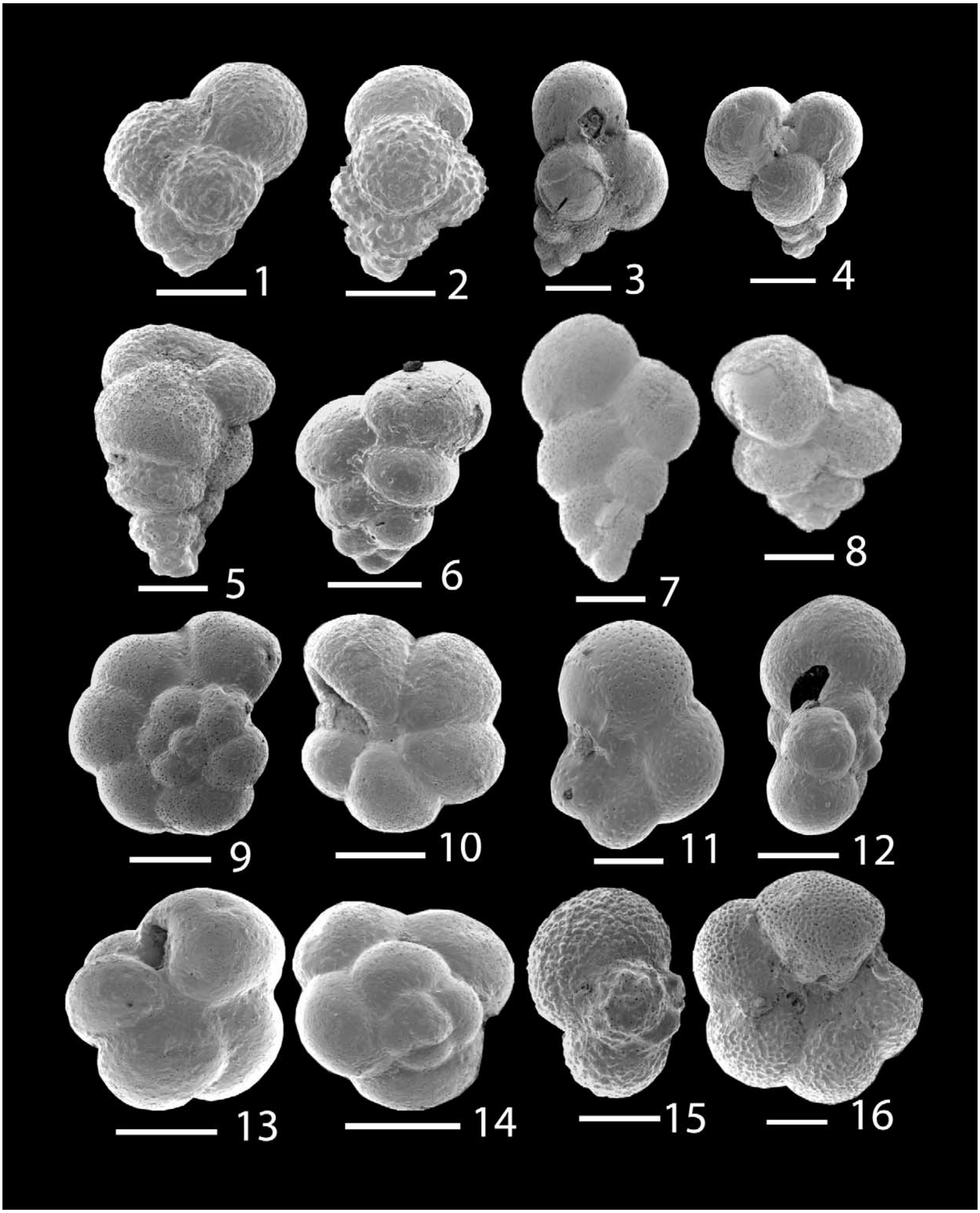

Plate II.

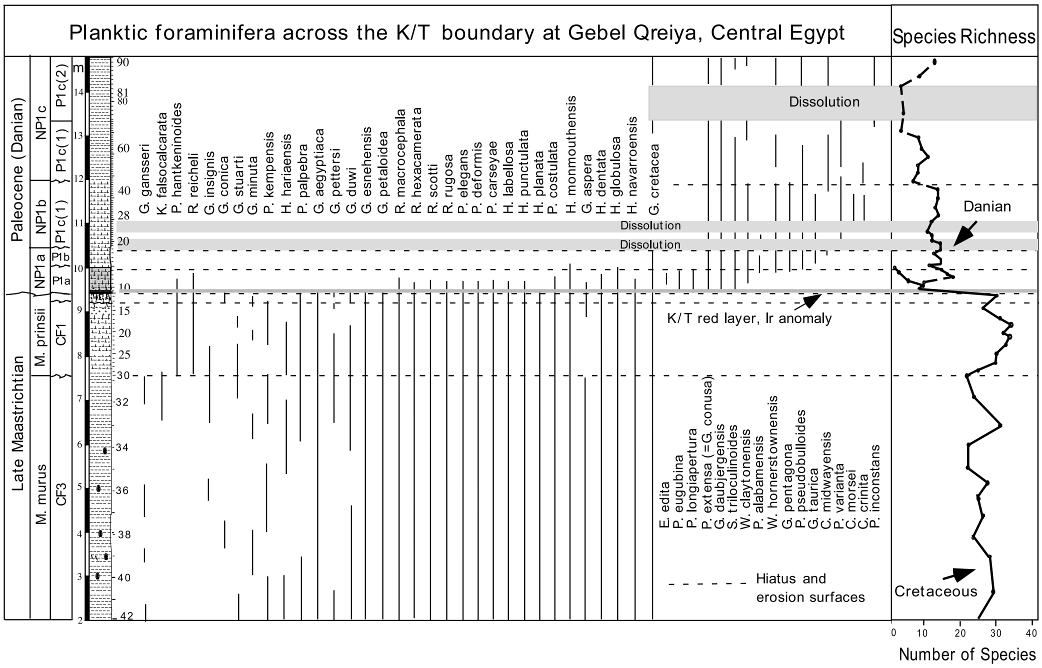

Fig. 5. Planktic foraminiferal species ranges at Gebel Qreiya, Egypt. Dashed lines mark hiatuses. Zone CF2 is missing (65.45–65.3 Ma), zone CF1 is only partially present, the earliest Danian zone P0 is restricted to the K/T red layer, the lower part of zone Pla is missing, hiatuses also mark zone Pla/b, Plb/Plc boundaries and within zone Plc. Note the overall low species richness in the late Maastrichtian is about half of normal Tethyan assemblages. Maximum species richness at Gebel Qreiya corresponds to the short warm event within the latest Maastrichtian zone CF1.

appearances of six Danian planktic foraminiferal species, including the zone Pla index species *Parvularugoglobigerina eugubina* and *P. longiapertura*, indicate that the earliest Danian zone P0 is restricted to the red layer (Fig. 5). In addition, the lower part of the overlying zone Pla is missing, as indicated by: (a) the absence of abundant *Guembelitria*, which are characteristic of the P0 and lower Pla zones, and (b) the presence of common Danian species in the > 63 μm size fraction which do not generally appear below the upper part of the *P. eugubina* zone or in Pla(2) (Keller et al., 1995, 2001). Moreover, the presence of abundant reworked Cretaceous species in the shale of zone Pla indicates erosion and redeposition under intensified current activity and/or shallower waters (Fig. 5).

Zone Pla(2) (*P. eugubina*) assemblages are

Plate II. Scale bar = 50 μm. Specimens 3 and 4 from the late Maastrichtian zone CF1. All other specimens from the early Danian zone Pla (*P. eugubina*) at Qreiya, Egypt.

1–4.	*Guembelitria cretacea*
5, 6.	*Woodringina hornerstownensis*
7.	*Chiloguembelina midwayensis*
8.	*Woodringina claytonensis*
9, 10.	*Parvularugoglobigerina eugubina*
11, 12.	*Parasubbotina varianta*
13, 14.	*Parvularugoglobigerina extensa* (= *Globoconusa conusa*)
15.	*Globoconusa daubjergensis*
16.	*Globigerina* (*Eoglobigerina*) *pentagona*

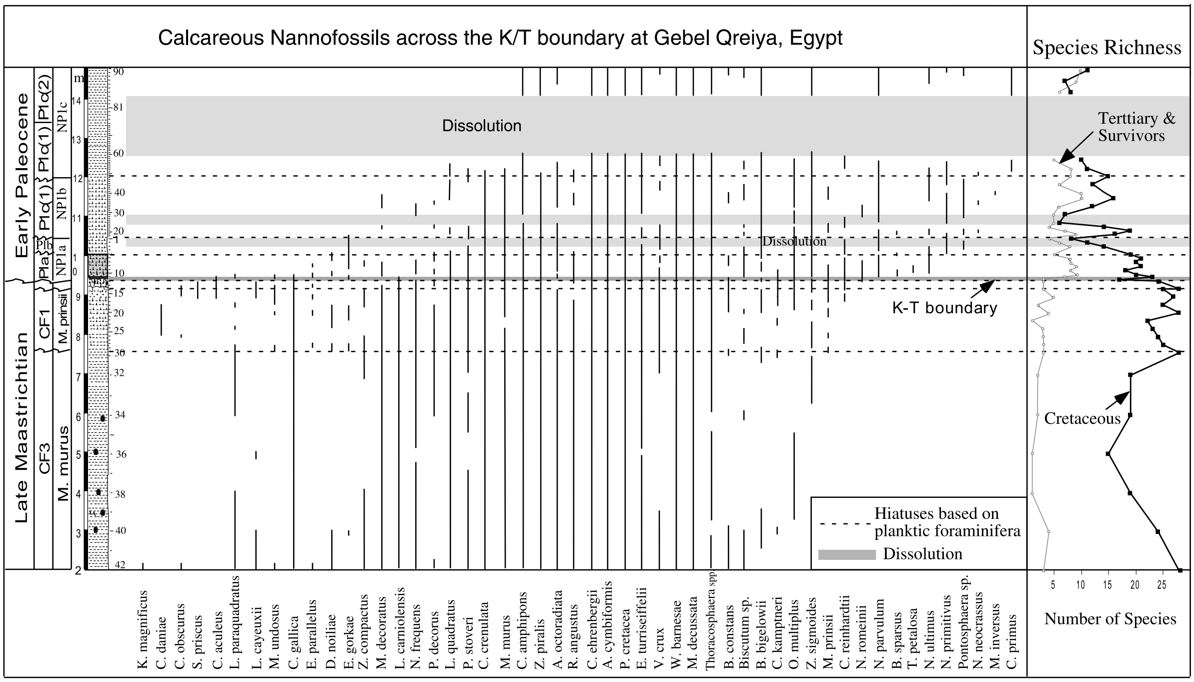

Fig. 6. Calcareous nannofossil species ranges and species richness at Gebel Qreiya, Egypt. Note the gradual decrease in Cretaceous species richness in the early Danian is partly due to reworked sediments. However, species that are considered as K/T survivors show a marked increase in their relative abundance in the early Danian.

present in the 50 cm-thick fissile dark gray shale that overlies the red clay and contains a well developed early Danian zone Pla assemblage that includes *Globoconusa daubjergensis*, *Parvularugoglobigerina eugubina*, *P. longiapertura*, *P. extensa* (= *G. conusa*), *Eoglobigerina edita* and *E. eobulloides*, followed by *Subbotina triloculinoides*, *S. trivialis* and *Woodringina claytonensis* (Fig. 5, Plates I and II). Calcareous nannofossils place this interval in zone NP1a (Fig. 6).

Zone Plb, the interval between the last occurrence of *P. eugubina* and/or *P. longiapertura* and the first appearance of *Parasubbotina varianta*, is condensed, partly due to dissolution and a hiatus as indicated by the abrupt disappearance of *P. longiapertura* immediately after its most abundant stage (53%), the peak abundance (63%) of *P. extensa* (formerly *G. conusa*), and the simultaneous first appearances of *P. alabamensis*, *Woodringina hornerstownensis*, and *Globanomalina taurica* (Fig. 5, Plate II). The calcareous nannofossil zone boundary NP1a/b coincides with this hiatus (Fig. 6).

Zone Plc, the interval between the first appearance of *Parasubbotina varianta* to the first appearance of *Praemurica trinidadensis*, marks the top 5 m of the section analyzed.

Zone P1c is divided into P1c(l) and P1c(2) based on the first appearance of *Praemurica inconstans* (Fig. 4), which first appears about 3.8 m above the K/T boundary and just below an interval of carbonate dissolution (Figs. 5 and 6). There are abrupt faunal assemblage changes within Plc(l) that indicate another hiatus at 2.5 m above the K/T boundary. Evidence for this hiatus includes (a) a sharp lithological break from marly shale to shale, (b) the abrupt disappearance of abundant *G. cretacea* and *G. daubjergensis*, and (c) the abrupt abundance decrease in *W. calytonensis*, *W. hornerstownensis*, *G. pentagona* and *P. varianta*. The calcareous nannofossil zone boundary NP1b/c coincides with this hiatus (Fig. 6).

Few planktic foraminifera or calcareous nannofossils are present in the interval above the carbonate dissolution in zones Plc(2) and NP1c (Figs. 5 and 6).

The hiatuses identified at Gebel Qreiya have also been identified in Israel, southern Tunisia, Bulgaria, Italy, Spain, Mexico, Guatemala and many deep-sea sections (e.g. MacLeod and Keller, 1991; Keller and Benjamini, 1991; Canudo et al., 1991; Keller et al., 1994, 1998, 2002; Luciani, 1997, 2002; Stinnesbeck et al., 1997; Adatte et al., 2002a,b). These hiatuses are generally associated with climate cooling, lower sea levels and intensified bottom circulation.

5. Stable isotopes

Foraminifera are relatively well preserved at Gebel Qreiya. However, even well preserved tests tend to be partially recrystallized with up to 50% diagenetic calcite (Pearson et al. (2001). Recrystallization of foraminiferal tests occurs upon settling in the cool waters of the ocean floor. As a result, oxygen isotopes tend to shift towards more positive (cooler) values and carbon isotopes towards more negative values (lower productivity). Isotopic values are thus biased towards cooler temperatures and lower productivity even in well preserved foraminiferal tests. However, carbon and oxygen isotope differentials between species tend to be retained during diagenesis, but with the effect of reducing the differential depending on the degree of diagenesis. Thus, in completely recrystallized tests, $\delta^{13}C$ values of benthic and planktic species converge (Pearson et al., 2001).

Since oxygen isotopic values are more sensitive to post-depositional alteration than carbon isotope values, no paleotemperature data can be obtained, although climatic trends are generally preserved. At Gebel Qreiya $\delta^{18}O$ values of *Rugoglobierina rugosa* vary, with an average about 2.0‰ lighter as compared with El Kef, Tunisia (Keller and Lindinger, 1989; Li et al., 2000), partly due to diagenetic alteration and partly to the shallower water depth at Qreiya (middle neritic as compared with outer neritic to upper slope at El Kef) and hence warmer waters. This study is primarily concerned with variations in primary productivity as reflected in surface-to-deep gradient changes in $\delta^{13}C$, and in evaluating the left and right coiling individuals of *Cibicidoides pseudoacutus* as potential environmental indicators.

5.1. *Sinistral and dextral coiling Cibicidoides pseudoacutus*

We have analyzed monospecific samples of the benthic foraminifer *Cibicidoides pseudoacutus* and the surface-dwelling planktic foraminifer *Rugoglobigerina rugosa* for the Maastrichtian. *Cibicidoides pseudoacutus* is frequently used for stable isotope analyses in continental shelf-slope sections. Recently, Coccioni and Galeotti (1998) and Galeotti and Coccioni (2002)) reported that sinistral coiling individuals dominated during climatic cooling immediately after the K/T boundary event, whereas dextral coiling individuals dominated during warmer periods, although they provided no supporting stable isotope data for individuals with different coiling directions. They concluded that the brief interval of dominantly sinistral individuals provides evidence for a prolonged period of nuclear winter following the K/T impact. In order to test this hypothesis we have separately analyzed samples of sinistral and dextral coiling individuals at El Kef and Gebel Qreiya. At El Kef, the test site of Coccioni and Galeotti (1998), we confirmed a predominance of sinistrally coiled individuals within the basal 15 cm of the boundary clay (zone P0, Fig. 7). However, $\delta^{18}O$ and $\delta^{13}C$ values show no significant variations between individuals with different coiling directions. In most samples isotopic values of sinistral and dextral individuals deviate less than 0.1‰ (Fig. 7, Table 3). In addition, there is no consistent correlation between samples with abundant sinistral individuals and cooling, though the overall pattern is intriguing for the immediate post-K/T interval.

At Gebel Qreiya we analyzed sinistral and dextral coiling individuals spanning climatic fluctuations from the late Maastrichtian zone CF3 (~66.8 Ma) through the Danian zone Plc (~64 Ma). As at El Kef, dextral and sinistral coiling individuals covary throughout the section. $\delta^{13}C$ and $\delta^{18}O$ values deviate an average of 0.2‰,

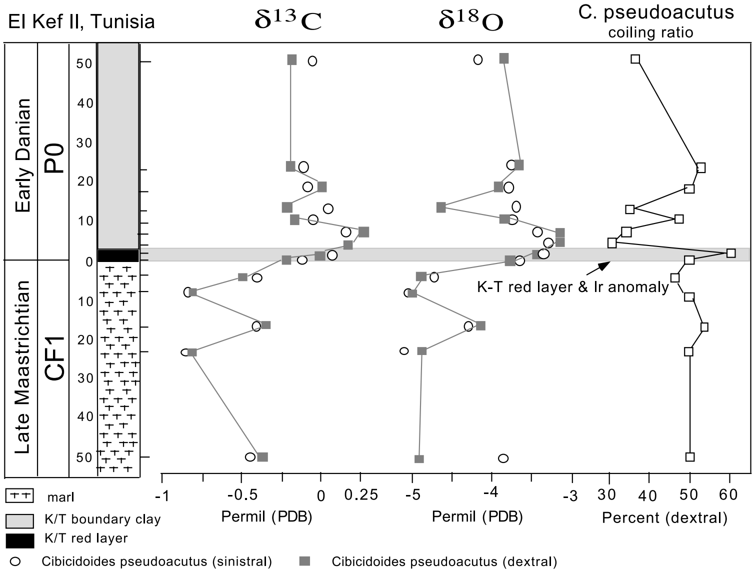

Fig. 7. Stable isotope values of sinistral and dextral coiling individuals of the benthic species *Cibicidoides pseudoacutus* and its coiling ratio across the Cretaceous–Tertiary boundary at El Kef, Tunisia. Note that coiling direction appears to be unrelated to temperature changes and that the relative abundance of sinistral coiling individuals does not correspond with tempearature changes as suggested by Galeotti and Coccioni (2002), though there seems to be a correlation with productivity.

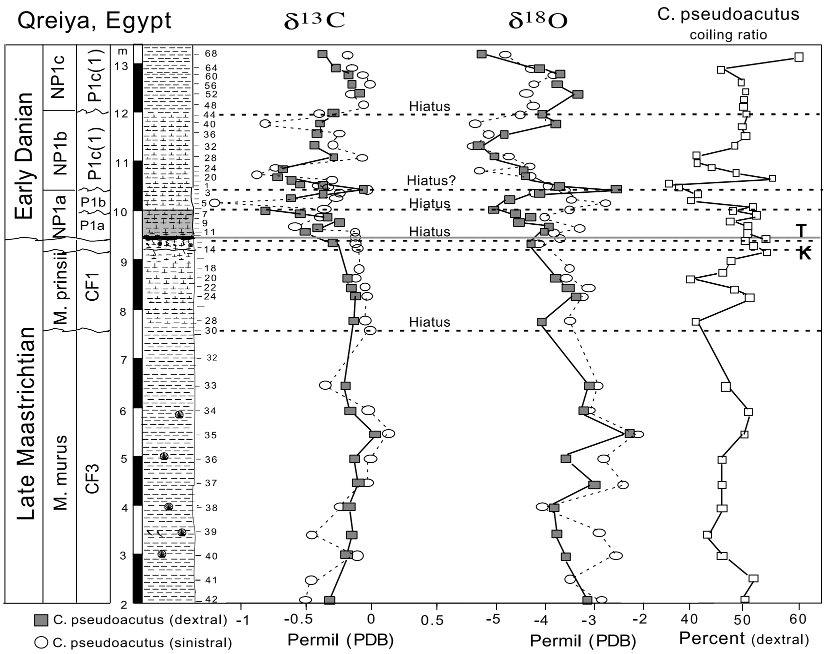

Fig. 8. Stable isotope values of sinistral and dextral coiling individuals of the benthic species *Cibicidoides pseudoacutus* and its coiling ratio during the late Maastrichtian and early Danian at Gebel Qreiya, Egypt. Note that sinistral and dextral coiling individuals show similar values and that there is no correlation between cooling and higher abundances of sinistrally coiled individuals as suggested by Galeotti and Coccioni (2002), except for an interval in zone Plb.

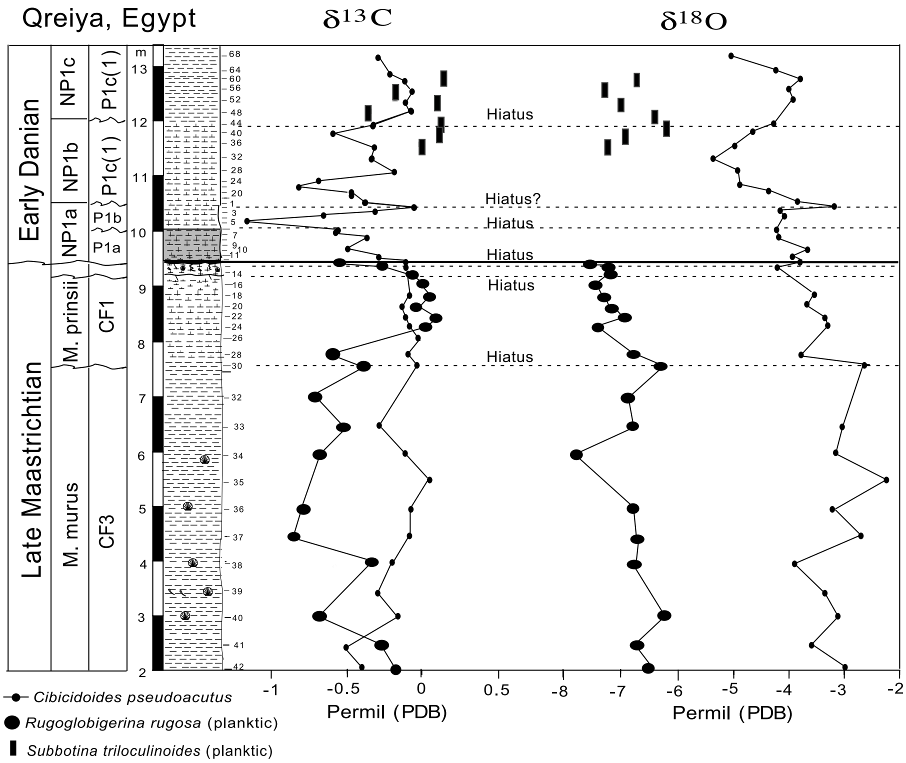

Fig. 9. Stable isotope values of averaged dextral and sinistral coiling individuals of the benthic species *C. pseudoacutus* and planktic species *Rugoglobigerina rugosa* at Gebel Qreiya, Egypt. Note the inverse surface-to-deep $\delta^{13}C$ gradient in zone CF3 (*M. murus*) that indicates a Strangelove ocean with surface productivity lower than in bottom waters, similar to that characteristically observed at the K/T boundary in low to middle latitudes. Oxygen isotopes indicate cooler temperatures in zone CF3 with respect to CF1, and higher though fluctuating temperatures in the early Danian followed by cooling in zone Plc. Note that these bottom water temperature trends may reflect the shallow, though fluctuating early Danian marginal sea, rather than climate trends.

with deviation greater in oxygen isotope values (Fig. 8). There appears to be no systematic isotopic difference between individuals with different coiling directions, although sinistral coiling individuals record more often slightly heavier $\delta^{18}O$ values during the late Maastrichtian and early Danian, but this trend is reversed in Plc. The coiling ratio of *C. pseudoacutus* fails to show a consistent relationship with climatic trends. In general, sinistrally coiled individuals more often predominate during warmer intervals than dextrally coiled individuals. There is only one interval in Plb where cooling coincides with abundant sinistrally coiled individuals (Fig. 8). Our data thus fail to support the hypothesis that sinistrally coiled individuals indicate climatic cooling. The increased abundance of sinistrally coiled individuals in the basal 15 cm of the boundary clay at El Kef and a similar increase in zone Plb at Qreiya appear to be anomalies related to environmental factors other than temperature. Instead, coiling direction in *C. psuedoacutus* appears to be related to primary productivity. This is suggested by the coincidence of high abundance of sinistrally coiled specimens at the base of the Danian (P0) and in Plb, the two intervals with lowest $\delta^{13}C$ values, indicating lowest productivity (e.g. Magaritz et al., 1992; Barrera and Keller, 1994).

5.2. Productivity and temperature trends

In view of the closely similar isotopic values obtained for dextral and sinistral coiling individuals of *C. pseudoacutus*, there appears to be no need for separate analyses by coiling direction. We have therefore averaged these values for Ge-

Table 1
Stable isotopes of left and right coiling *Cibicidoides pseudoacutus* at Gebel Qreiya, Egypt

No.	Depth (m)	*C. Pseudoacutus* left coiling $\delta^{13}C$	*C. Pseudoacutus* left coiling $\delta^{18}O$	*C. Pseudoacutus* right coiling $\delta^{13}C$	*C. Pseudoacutus* right coiling $\delta^{18}O$	^{13}C	^{18}O	% Species left coil
90	14.95	0.70	−3.82	−0.48	−4.79	1.18	0.97	53
87	14.65	0.06	−2.70	−0.26	−4.16	0.32	1.46	52
68	13.15	0.19	−4.81	−0.38	−5.32	0.57	0.51	40[a]
64	12.95	0.16	−4.26	−0.28	−4.20	0.44	0.06	54
60	12.75	0.09	−3.91	−0.15	−3.68	0.24	0.23	68[a]
56	12.55	0.01	−4.20	−0.14	−3.63	0.15	0.57	49
52	12.35	−0.17	−4.46	−0.08	−3.35	0.25	1.11	49
48	12.15	−0.07	−4.24					50
44	11.95	−0.41	−4.55	−0.30	−4.05	0.11	0.50	49
40	11.75	−0.81	−5.58	−0.38	−3.75	0.43	1.83	50
36	11.55	−0.26	−5.09	−0.42	−4.94	0.16	0.15	49
32	11.30	−0.29	−5.29	−0.46	−5.22	0.17	0.07	52
28	11.10	−0.08	−4.86	−0.30	−5.01	0.22	0.15	57
24	10.90	−0.39	−3.92					57
22	10.80	−0.88	−5.39	−0.72	−4.48	0.16	0.91	56
20	10.70	−0.29	−4.40	−0.67	−4.45	0.38	0.05	52
18	10.60	−0.34	−5.04					44
1	10.50	−0.44	−3.92	−0.40	−3.21	0.04	0.71	63
2	10.40	−0.04	−3.56	−0.04	−2.51	0.00	1.05	61
3	10.30	−0.25	−4.37	−0.36	−4.23	0.11	0.14	57
4	10.20	−0.28	−3.50	−0.66	−4.82	0.38	1.32	59
5	10.10	−1.21	−2.80					49[a]
6	10.00	−0.37	−3.51	−0.87	−5.06	0.50	1.55	52
7	9.90			−0.58	−4.60			48
8	9.80	−0.36	−4.02	−0.30	−4.33	0.06	0.31	54
9	9.70			−0.26	−4.53			49
10	9.60	−0.59	−3.25	−0.39	−3.95	0.20	0.70	49
11	9.50	−0.11	−3.80	−0.51	−4.00	0.30	0.20	46
12	9.40	−0.11	−3.73					50
13	9.30	−0.11	−4.07	−0.34	−4.27	0.23	0.20	48
14	9.20	−0.10	−2.83					45
16	9.00							52
18	8.80	−0.10	−3.51					54
20	8.60	−0.12	−3.54	−0.19	−3.86	0.07	0.32	59
22	8.40	−0.06	−3.09	−0.18	−3.55	0.12	0.46	52
24	8.20	−0.05	−3.26	−0.13	−3.44	0.08	0.18	49
26	8.00			0.01	−1.95			44[a]
28	7.80	−0.08	−3.49	−0.15	−4.09	0.07	0.60	58
30	7.60	−0.01	−2.54					49
31								few
32								few
33	6.50	−0.37	−2.99	−0.23	−3.10	0.14	0.11	54
34	6.00	−0.03	−3.08	−0.19	−3.21	0.16	0.13	51
35	5.50	0.15	−2.04	0.03	−2.30	0.12	0.26	52
36	5.00	−0.04	−2.88	−0.10	−3.59	0.06	0.71	55
37	4.50	−0.05	−2.37	−0.15	−3.00	0.10	0.63	55
38	4.00	−0.25	−4.14	−0.20	−3.78	0.05	0.36	54
39	3.50	0.49	−2.97	−0.19	−3.84	0.68	0.87	57
40	3.00	−0.13	−2.55	−0.21	−3.61	0.08	1.06	55
41	2.50	−0.49	−3.56					50
42	2.00	−0.53	−2.90	−0.33	−3.14	0.20	0.14	52

[a] Percent based on less than 100 specimens.

Table 2
Stable isotopes of planktic foraminifera *Rugoglobigerina rugosa* and *Subbotina triloculinoides* at Gebel Qreiya, Egypt

Species	No.	Depth (m)	$\delta^{13}C$
Maastrichtian (> 150 μm)			
R. rugosa	11	9.50	−0.08
R. rugosa	12	9.40	−0.57
R. rugosa	13	9.30	−0.24
R. rugosa	14	9.20	−0.08
R. rugosa	16	9.00	0.00
R. rugosa	18	8.80	0.04
R. rugosa	20	8.60	−0.07
R. rugosa	22	8.40	0.11
R. rugosa	24	8.20	0.03
R. rugosa	26	8.00	0.55
R. rugosa	28	7.80	−0.63
R. rugosa	30	7.60	−0.44
R. rugosa	32	7.40	−0.72
R. rugosa	33	6.50	−0.51
R. rugosa	34	6.00	−0.70
R. rugosa	36	5.00	−0.78
R. rugosa	37	4.50	−0.91
R. rugosa	38	4.00	−0.32
R. rugosa	40	3.00	−0.70
R. rugosa	41	2.50	−0.21
R. rugosa	42	2.00	−0.17
Danian (100–150 μm)			
S. triloculinoides	90	14.95	−0.12
S. triloculinoides	87	14.65	−0.13
S. triloculinoides	60	12.75	0.15
S. triloculinoides	56	12.55	−0.14
S. triloculinoides	52	12.35	0.09
S. triloculinoides	48	12.15	−0.36
S. triloculinoides	44	11.95	0.11
S. triloculinoides	40	11.75	0.12
S. triloculinoides	36	11.55	0.00

bel Qreiya in each sample to obtain overall $\delta^{13}C$ and $\delta^{18}O$ trends (Fig. 9). The data show strong surface and bottom water trends that are largely consistent with coeval eastern Tethys isotopic records of the same species (Keller and Lindinger, 1989; Stueben et al., 2002), except for the surface-to-deep carbon isotope gradient.

The late Maastrichtian surface-to-deep $\delta^{13}C$ gradient of the benthic foraminifer *Cibicidoides pseudoacutus* and planktic foraminifer *Rugoglobigerina rugosa* at Qreiya is very unusual. Benthic $\delta^{13}C$ values show relatively minor variations between 0‰ and −0.3‰, though there are major excursions in planktic $\delta^{13}C$ values (Fig. 9). Near the base of the section, a small positive surface-to-deep $\delta^{13}C$ gradient is present. This is followed by a negative planktic $\delta^{13}C$ excursion of 0.5–0.8‰ and establishes an inverse surface-to-deep gradient for the remainder of zone CF3 and into the base of CF1 (Fig. 9, Tables 1 and 2). A positive shift of 0.8‰ in planktic $\delta^{13}C$ values re-establishes a slightly positive surface-to-deep gradient in zone CF1. Near the top of the Maastrichtian (top 20 cm), planktic $\delta^{13}C$ values drop by 0.6‰ and are again more negative than benthic values, as is characteristic of the K/T boundary.

Is the observed reversal in the surface-to-deep gradient real or an artifact of diagenesis? Recrystallization of foraminiferal tests occurs in the cooler waters of the ocean floor, which shifts planktics towards more negative carbon values than benthic species, and hence reduces the surface-to-deep gradient. Total (100%) recrystallization would result in convergence of planktic and benthic values (Pearson et al., 2001). Thus, recrystallization alone cannot account for the more negative planktic values during the late Maastrichtian at Qreiya, and strongly suggests that surface productivity was very low. The unusual high-stress planktic foraminiferal assemblages dominated by *Guembelitria* and small *Heterohelix* species support this interpretation.

Benthic $\delta^{13}C$ values show only a minor decrease

Table 3
Stable isotopes of left and right coiling benthic foraminifera *Cibicidoides pseudoacutus*, at El Kef, Tunisia

Depth	left coiling		right coiling	
(cm)	$\delta^{13}C$	$\delta^{18}O$	$\delta^{13}C$	$\delta^{18}O$
+50	−0.06	−4.12	−2.22	−3.88
+10–23	−0.12	−3.76	0.21	−3.65
+15–20	−0.08	−3.74	0.00	−3.94
+10–15	0.04	−3.67	−0.25	−4.61
+7–13	−0.04	−3.76	−0.02	−3.77
+6–8	0.12	−3.47	0.26	−3.17
+2–4	0.32	−3.31	0.16	−3.17
+1–2	0.06	−3.43	−0.02	−3.45
0–1 K/T	−0.13	−3.60	−0.23	−3.76
−1–5	−0.41	−4.72	−0.52	−4.91
−5–10	−0.69	−5.05	−0.67	−5.03
−15–20	−0.44	−4.28	−0.33	−4.14
−20–25	−0.77	−5.10	−0.65	−4.94
−50–55	−0.47	−4.34	−0.37	−4.97

(+) above K/T boundary, (−) below K/T boundary

(−0.3‰) across the K/T boundary, consistent with benthic patterns elsewhere (Keller and Lindinger, 1989; Zachos et al., 1989). However, in the early Danian Pla–Plb interval benthic values continued to drop and reached minimum values at the Pla/Plb hiatus (Fig. 9). The first recovery is indicated at the P1b/Plc boundary and hiatus by a brief positive excursion, followed by another negative excursion in the lower part of Plc(l). Similar positive and negative excursions were observed at these time intervals in the Negev (Magaritz et al., 1992) and South Atlantic (Stott and Kennett, 1990; Barrera and Keller, 1994), and various low latitude deep sea localities (Zachos et al., 1989; Keller and Lindinger, 1989).

Temperature trends indicate that relative to the late Maastrichtian zone CF1 and early Danian zone Plc(l), benthic and planktic $\delta^{18}O$ values suggest cooler temperatures during the late Maastrichtian zone CF3 (Fig. 9). This warming trend in zone CF1 is consistent with middle to high latitude climate trends between 65.4 and 65.2 Ma (CF1–2 interval, Li and Keller, 1998a). During the early Danian lower part of zone Plc, benthic $\delta^{18}O$ values indicate warmer temperatures, whereas planktic values suggest variably cooler conditions. The warmer bottom water at Gebel Qreiya likely reflects a shallowing and restricted sea. A lower sea level at this time has been observed on carbonate shelves of the southern Tethys (e.g. Guatemala, Fourcade et al., 1998; Stinnesbeck et al., 1997). Cooler temperatures beginning in the lower part of Plc(l) parallel increased $\delta^{13}C$ values and the recovery of normal primary productivity in the middle and low latitude ocean. Although these data provide a glimpse of early Danian climate changes, this interval is still poorly understood because of incomplete stratigraphic records, diagenetic alteration, and the absence of long-ranging planktic species for isotopic analyses of surface waters.

6. Mineralogy

6.1. Bulk rock

During the late Maastrichtian at Gebel Qreiya, sediments were dominated by calcite, phyllosilicates, quartz and plagioclase. In the lowermost 2 m of the section (base of zone CF3), calcite deposition averages ∼70%, quartz 3%, and phyllosilicates vary between 15 and 25%, suggesting relatively low energy conditions (Fig. 10). A significant change occurs between 2 and 7.5 m (upper 2/3 of zone CF3), where calcite decreases to 40%, phyllosilicates increase to 40–45%, and detritus (quartz and plagioclase) increases to 5–6%. This suggests increased erosion and runoff associated with a lower sea level, as also indicated by a hiatus (CF3/CF1 zones) and the presence of macrofossils. In the 2 m below the K/T boundary (zone CF1), deposition of calcite is high again (60–70%, except for two isolated samples that were not analyzed for foraminifera), and phyllosilicates low (20–30%), followed by a reversed trend in the 1 m below the K/T boundary (Fig. 10). These data suggest decreased detrital influx during a relatively higher sea level and globally warmer climate indicated by oxyen isotope data at Qreiya (Fig. 9) and elsewhere (Stott and Kennett, 1990; Li and Keller, 1998a–c; Olsson et al., 2001).

There are also strong Danian trends in bulk rock compositions. The early Danian interval of zone Pla (*Parvularugoglobigerina eugubina*) is relatively high in calcite (∼45%) and phyllosilicates (∼45%), and low in quartz (∼2.5%). This high calcite content is inconsistent with the very low foraminiferal numbers, but can be explained by the presence of common reworked Cretaceous species (Fig. 5). Upsection, calcite decreases to a variable 20–30% and dropped to near 0% in a dissolution interval at the Plc(l)/Plc(2) zone boundary where foraminifera and nannofossils are absent (Figs. 5 and 6). At the same time, phyllosilicates gradually increase to a maximum of 80%, and detrital input is variable (3–4% quartz, 1% K-feldspar, 1–1.5% plagioclase), suggesting increased erosion and transport, as also indicated by several short hiatuses (Fig. 5).

6.2. Clay minerals

At Qreiya, the main clay phases are kaolinite (55–85%), smectite (10–30%), chlorite (5–25%)

and illite (2–15%, Fig. 11). The smectite presence implies that the clay minerals are not transformed due to burial diagenesis, and smectites are therefore mostly of detrital origin as a result of local uplift and/or variations in weathering processes and soil formation in the bordering continental areas (Chamley, 1989; Weaver, 1989). Clay mineral compositions remain relatively stable in zone CF3, with kaolinite dominant (68–78%), common smectite (9–16%) and chlorite (10–18%), and minor amounts of illite (< 3%). The base of zone CF1 is marked by fluctuating but decreasing smectite and kaolinite, with 10% and 59%, respectively, and increasing mica (> 3%) and chlorite (up to 25%). Above this interval in CF1, kaolinite (60–70%) and smectite (15–25%) increase, whereas chlorite (7–14%) decreases. Across the K/T boundary (top of CF1 and Pla, Fig. 11) mica and chlorite increase and kaolinite decreases along with the smectite/chlorite+mica and kaolinite/smectite ratios. Above this interval kaolinite gradually increases and reaches maximum values (76–88%) at the base of P1b, whereas smectite, mica and chlorite decrease. Near the top of the section (zone Plc(2)), smectite increases (29%), kaolinite remains relatively stable (65–75%), whereas chlorite (< 10%) decreases.

6.2.1. Interpretation

During the late Cretaceous, Gebel Qreiya was located near the paleoequator (Smith et al., 1994),

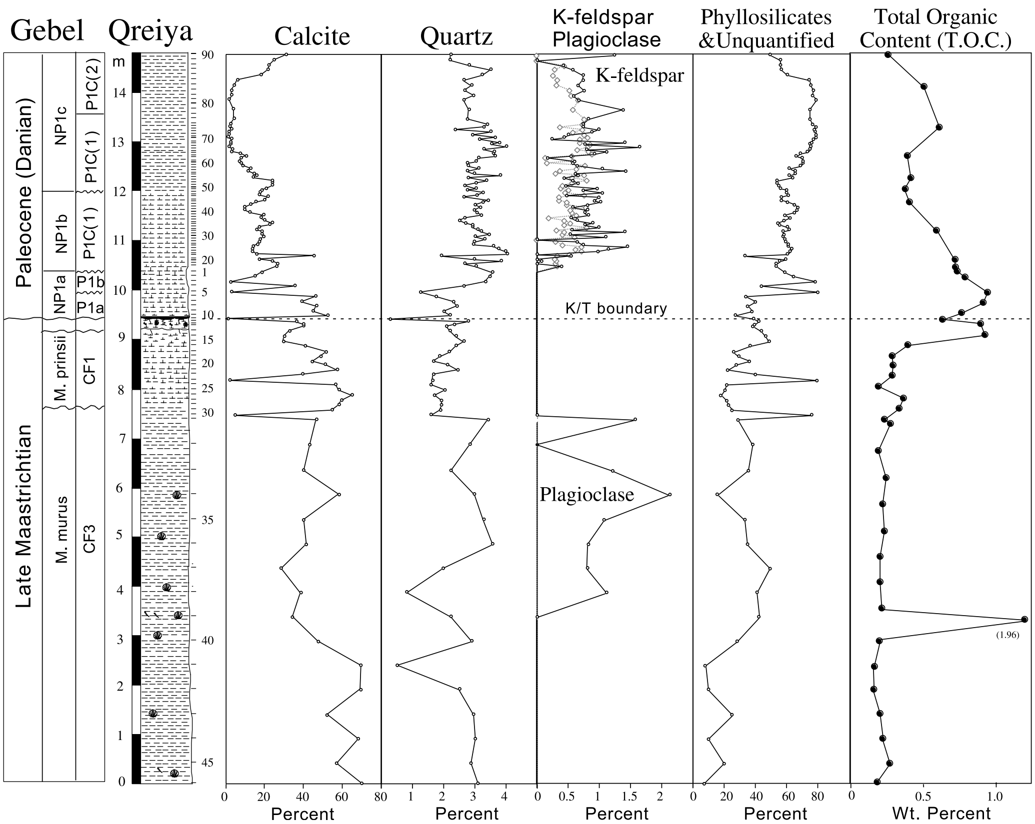

Fig. 10. Bulk rock composition and total organic carbon (TOC) at Gebel Qreiya, Egypt. Note that the unusually high calcite content immediately above the K/T boundary is the result of abundant reworked Maastrichtian foraminifera in this interval. High TOC values across the K/T boundary most likely reflect increased erosion and runoff. HI and OI indices indicate that the organic matter is of terrigenous origin and may have been oxidized and partly altered during erosion and transport. See text for discussion.

as also indicated by the high abundance of kaolinite, which is a weathering product in subtropical to tropical environments where perennial rainfall and mean annual soil temperatures exceed 15°C (Gaucher, 1981). Dominance of kaolinite was also observed in Tunisia (Li et al., 2000; Adatte et al., 2002a,b). At Qreiya, warm wet, tropical and subtropical late Maastrichtian conditions characterized by low seasonality contrasts and predominantly chemical weathering are suggested by the high kaolinite, moderate smectite, and low mica and chlorite contents (Fig. 11). The presence of crystallized mica, characterized by a large XRD peak also indicates that active chemical weathering prevailed during the late Maastrichtian and in the early Danian. Wet humid conditions are also indicated by the presence of *Tricopolites reticulates* (comparable to the genus *Gunnera*) in nearby sections, a genus which is restricted to environments of heavy rainfall and higher elevations (>750 m, Schrank, 1984).

Smectite at Qreiya is variable but gradually increases from the bottom to the top of the section. Smectite in marine sediments may have several origins. Detrital smectite eroded from suitable soils, typically with fine grain sizes, may preferentially settle in distal open marine environments, whereas chlorite, kaolinite and mica are deposited closer to the shoreline (Porrenga, 1966; Gibbs, 1977; Adatte and Rumley, 1989). In the absence of other changes, detrital smectite in marine sediments increases during sea-level highstand periods, whereas kaolinite, chlorite and mica increase during lowstand periods. The presence of abundant smectite is generally linked to transgressive seas and warm climate with alternating humid and arid seasons, but can also reflect volcanic activity (Chamley, 1989, 1998; Deconinck and

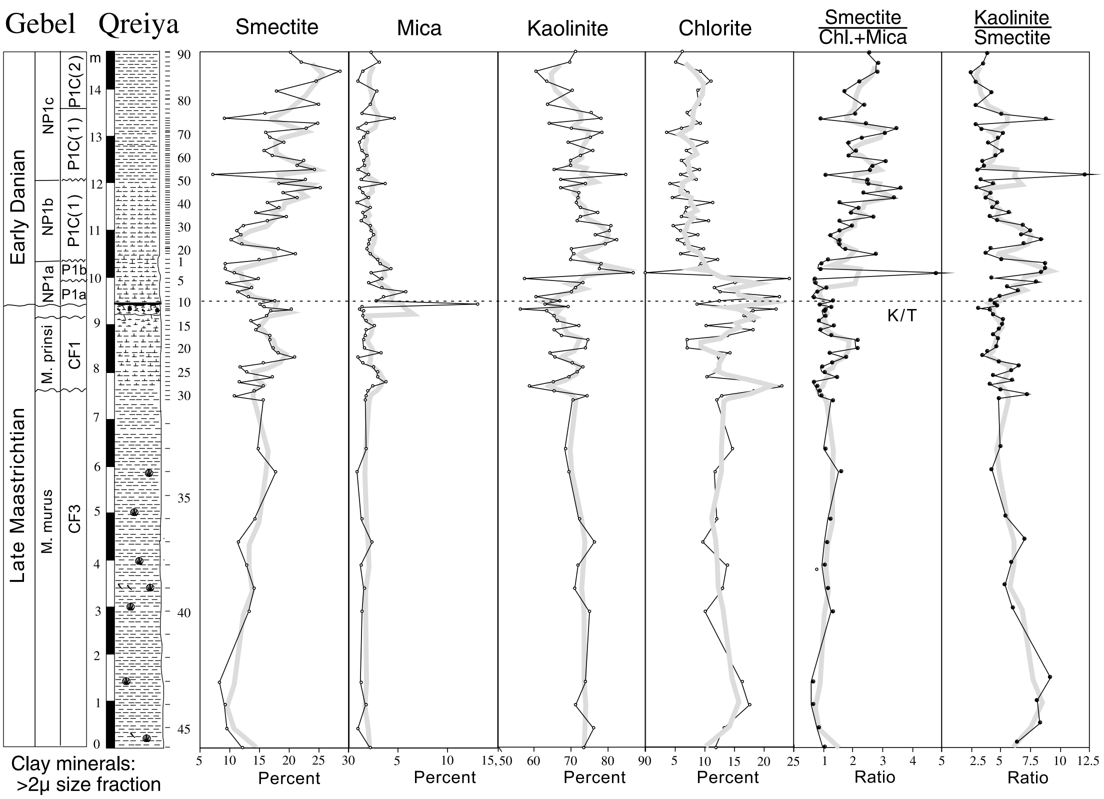

Fig. 11. Clay mineral content at Gebel Qreiya, Egypt. The main clay phases are kaolinite and smectite, suggesting a mostly detrital origin as a result of uplift and/or variations in weathering processes and soil formation in bordering continental areas. The high abundance of kaolinite suggests a warm, wet, tropical to subtropical environment. See text for discussion.

Chamley, 1995). At Qreiya the overall increase in smectite during the early Danian reflects the increasing sea-level trend that has been documented from many sections in Egypt (e.g. Schnack and Luger, 1998; Tantawy et al., 2001). Major variations in smectite abundance coincide with hiatuses at the CF3/CF1, CF1/P0, P1a/P1b intervals and generally correspond to increases in chlorite and mica to the detriment of smectite and kaolinite, and hence indicate significant mechanical erosion of nearby areas. The coeval increase in smectite and chlorite observed in the topmost Maastrichtian may also indicate drier conditions (seasonality) in elevated areas (Figs. 11 and 12).

The kaolinite/smectite ratio is a climate proxy that reflects humid/warm to more dry and seasonal climate variations (e.g. Robert and Chamley, 1991; Robert and Kennett, 1992). The ratio of kaolinite to smectite (K/SM) can therefore be used as proxy for climate change. Based on this proxy, perennially humid conditions prevailed in central Egypt during the late Maastrichtian and early Danian except for two intervals with drier, more seasonally humid climates during the latest Maastrichtian and in the early Danian zone Plc(2) (Fig. 12).

6.3. Total organic carbon

Organic carbon and Rock-Eval pyrolysis data indicate that throughout CF3, TOC values rarely exceed 0.25 wt%, with average values about 0.22 wt% (Fig. 10). The highest TOC values (1.96%) occur in a single sample (Nr. 39) in the lower part of zone CF3 (Fig. 10). Although this peak value is anomalous within the otherwise low TOC content, planktic foraminiferal data show a major increase in low oxygen-tolerant heterohelicids in this sample (Keller, in press), which suggests an influx of nutrient-rich waters and expansion of the oxygen minimum zone. In the lower and middle parts of zone CF1, TOC values remain low, but increase rapidly to a maximum of 0.96% within the upper part. This interval, bounded by two erosion surfaces, also contains gastropod and bivalve shells and suggests increased erosion and transport from shallower areas, as also indicated by bulk rock minerals. TOC values decrease to 0.6% in the K/T red layer, but gradually increase to a mximum of 0.94% at the P1a/P1b hiatus and remain high in P1b with average values of 0.75% (Fig. 10).

The kerogens present at Gebel Qreiya are thermally immature, as indicated by the low to slightly elevated T_{max} values between 415 and 425°C. The pyrolysis data further suggest a terrigenous source (Type III or IV), high sediment dilution and perhaps oxidizing bottom water conditions. However, post-depositional alteration is also indicated by the low hydrogen index (HI) (20–30 HC/g TOC) and high oxygen index (OI) values (180–200 mg CO_2/g TOC). The upper part of CF3 exhibits very high OI values (1500–3000 mg CO_2/g TOC) and suggests that the main part of the organic matter in the shale could have been altered and partly destroyed. Thus, because of post-depositional alteration, TOC values provide no clues to the origin of the very low surface productivity values observed in carbon isotope values.

7. Discussion

7.1. Hiatuses

Biostratigraphic analyses of the Gebel Qreiya section based on planktic foraminifera and calcareous nannofossils indicate that late Maastrichtian to early Danian sediment deposition was interrupted repeatedly by erosion and non-deposition related to sea-level regressions and tectonic activity (Figs. 3 and 12). As a result, all of the planktic foraminiferal and calcareous nannofossil biozones are incomplete due to hiatuses (Figs. 5 and 6). Short hiatuses can be recognized in the latest Maastrichtian between zones CF3/CF1 (*M. murus*/*M. prinsii*) and within CF1 just below the K/T boundary based on erosional surfaces, lithological, geochemical and mineralogical changes, and faunal assemblage and species abundance variations. These hiatuses coincide with local tectonic activity (Klitzsch and Wycisk, 1987) and climate and sea-level fluctuations. For example, the late Maastrichtian climatic cooling that culminated at 65.5 Ma with a major sea-level drop coincides with the major CF3/CF1 hiatus. The subsequent short warm event between 65.4 and 65.2 Ma (zone CF1), followed by gradual cooling during the last 100 000 years of the Maastrichtian (Li and Keller, 1998a,c), coincides with an erosional surface near the top of CF1 (Figs. 3 and 5). The 1 cm-thin K/T boundary red clay layer and Ir anomaly also overlies an undulose, burrowed, erosional surface that marks another hiatus or condensed interval. Above the red clay, the lower part of zone Pla (Pla(l) is missing. Short hiatuses are also present between zones Pla/Plb, Plb/Plc and within Plc(l).

In the fossil record, these hiatuses can be recognized by the simultaneous first or last appearances of several species which normally appear sequentially, the absence of certain acme peaks (e.g. *Guembelitria* peak in the earliest Danian), the absence of the characteristically tiny (<63 μm) earliest Danian fauna, and the abrupt disappearances or first appearances of new species with abundant well developed specimens that are known to appear at a later evolutionary transition. In the field, hiatuses can often be recognized by hardgrounds, undulating erosional surfaces, truncated burrowed surfacs, macrofossils and lithological changes. In the mineralogical record, erosion and hiatuses are frequently apparent by sudden mineralogical changes and increased detrital influx. The hiatuses observed at Gebel Qreiya have also been observed in numerous K/T boundary sections, including the Negev, Israel, Tunisia, Bulgaria, Denmark, Spain, Mexico, Haiti and deep sea sites (e.g. MacLeod and Keller, 1991; Canudo et al., 1991; Keller and Benjamini, 1991; Shahin, 1992; Keller, 1993; Samir, 1994; Keller et al., 1993; 1994; 1998, 2001; Apellaniz et al., 1997; Luciani, 1997). Sea-level lowstands accompanied by intensified bottom water circulation are most likely responsible for these hiatuses, though locally tectonic activity may significantly contribute to erosion, as was likely the case in central Egypt (Schnack and Luger, 1998).

7.2. Sea level and climate

The late Maastrichtian climate record is well known from studies in the Tethys, equatorial Pacific and the high latitudes (Brinkhuis and Zachariasse, 1988; Keller et al., 1993, 1995; Barrera, 1994; Barrera et al., 1997; Li and Keller, 1998a,c; Kucera and Malmgren, 1998). These records show that the Maastrichtian cooling trend reached its maximum at about 65.5 Ma, coincident with a sea-level lowstand and widespread hiatus (Baum and Vail, 1988; Donovan et al., 1988; Keller and Stinnesbeck, 1996; Li et al., 2000). At Gebel Qreiya, the equivalent interval is likely the hiatus between CF3 and CF1 (Figs. 3 and 12). This cold event was followed by rapid global warming of sea surface temperatures by 3–4°C in middle and high latitudes between 65.45 Ma and 65.20 Ma (Li and Keller, 1998c). This warm event is easily recognized in planktic foraminifera by increased abundance of tropical and subtropical species in low latitudes and maximum species diversity. At Gebel Qreiya, this warm event is at least partially present in CF1, marked by an abundance of *Plummerita hantkeninoides* (10–15%) and rugoglobigerinids (25–30%), maximum species richness, high calcite and kaolinite, and warmer surface water temperatures (Figs. 5, 9 and 12). Climate cooled gradually during the last 100 kyr of the Maastrichtian (Li and Keller, 1998c). This climatic cooling appears to be at least partly present at Gebel Qreiya in the top 50 cm of the Maastrichtian, as indicated by decreased abundance of rugoglobigerinids and *P. hantkeninoides*, decreased calcite and kaolinite and increased phyllosilicates, quartz, smectite, chlorite and TOC (Figs. 10 and 11).

The Danian climatic and sea-level records are more difficult to compare with other Tethyan sections because very little of the early Danian sediment record is preserved at Gebel Qreiya. In the most complete sections, such as the El Kef stratotype of Tunisia, the K/T boundary is marked by a 2–3‰ drop in surface water $\delta^{13}C$ values, suggesting greatly reduced productivity and climate cooling (Fig. 7). Climate remained cool, though fluctuating, whereas primary productivity did not recover until zone Plc (Keller and Lindinger, 1989; Zachos et al., 1989). Similar climatic and productivity changes are observed in the early Danian at Gebel Qreiya, where the return to a warmer climate and pre-K/T carbon-13 values

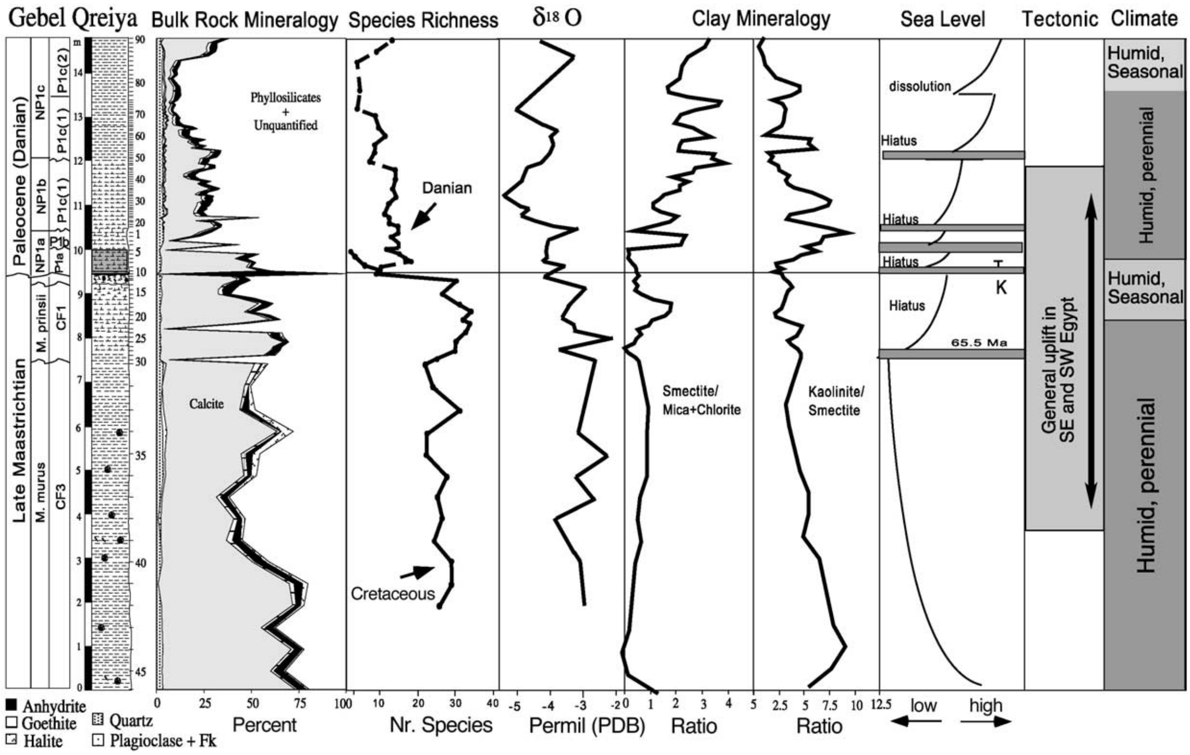

Fig. 12. Summary of paleoenvironmental indices, including bulk and clay mineralogy, stable isotopes, species richness, sea-level changes, climate and local tectonic activity at Gebel Qreiya, Egypt. Note that the late Maastrichtian to early Paleocene Asyut Basin in central Egypt was bordered by deltaic complexes to the south and experienced tectonic uplift that may have resulted in the formation of localized basins with restricted circulation leading to high-stress biotic conditions for marine plankton and low species richness. Note also that the observed hiatuses coincide with coeval erosion events globally and hence reflect a eustatic sea-level component that may have exacerbated erosion due to local tectonic activity.

was also delayed until the upper part of zone Plb, when kaolinite reached maximum values to the detriment of smectite and chlorite (Fig. 11).

7.3. Paleoenvironment of the Eastern Desert of Egypt

During the late Maastrichtian zone CF3 (66.8–65.5 Ma) the Eastern Desert of Egypt experienced the critical high-stress conditions that are usually associated with the K/T boundary event. Surface productivity dropped well below levels necessary to maintain the normal carbon isotopic gradient in the ocean, resulting in an inverse surface-to-deep gradient (Strangelove ocean). Species diversity dropped to less than half of normal faunal assemblages, and the opportunistic disaster species *Guembelitria* dominated (60–90%), though alternating with low oxygen-tolerant heterohelicids (*H. navarroensis, H. dentate*, *H. globulosa*, Fig. 5, Keller, 2002). The conditions that created this high-stress environment are likely related to local tectonic activity coupled with global climate and sea-level changes. Sediment deposition occurred in a middle to outer neritic (100–250 m) environment interrupted by erosion due to sea-level fluctuations (Fig. 12). Similar paleodepth environments in Tunisia, the Sinai or Negev retained normal species diversity, and the disaster species *Guembelitria* is rare or absent, except in two short intervals in the Negev which are marked by syntectonic activity (Almogi-Labin et al., 1990; Abramovich et al., 1998; Abdelmalik et al., 1978; Shahin, 1992).

To create the observed high-stress environment at Gebel Qreiya, local tectonic conditions, coupled with lower sea levels due to global sea-level regressions (at 66.8 and 66.5 Ma) may have temporarily isolated the Eastern Desert sea. In the south of Egypt, the late Maastrichtian (zone CF3) coincided with the onset of tectonic activity and the development of uplifted areas may have created semi-restricted basins with sluggish circulation, which in turn resulted in stagnant low oxygen conditions and decreased surface productivity that favored low species diversity and high-stress tolerant heterohelicid and guembelitrid species, as observed within zones CF3 and CF1 (Fig. 5, Keller, 2002). Alternatively, a lower sea level coupled with the deltaic conditions and increased evaporation in southern Egypt (Schnack and Luger, 1998; Schnack, 2000) may have significantly altered marine conditions (e.g. increased salinity, decreased oxygen) in the Asyut Basin, leading to the observed low surface productivity and low species diversity. The lower part of CF1 is associated with locally warmer temperatures, a rising sea level and global climate warming between 65.4 and 65.2 Ma, whereas the upper part is marked by cooling and a lower sea level (Li and Keller, 1998c).

During the early Danian, planktic foraminiferal populations and stable isotope data indicate that the depositional environment in the Eastern Desert was very similar to that of the Tethys region in general, though specific comparisons are difficult to make due to several hiatuses at Gebel Qreiya and the influence of local tectonic activity as suggested by a general increase in detritus (Fig. 10). This is evident by the unusually high calcite content in the very incomplete zone P1a as a result of reworked Cretaceous species, and the increased detrital influx in the early Danian. Since the early Danian is generally characterized by a gradually rising though fluctuating sea level (MacLeod and Keller, 1991; Keller and Stinnesbeck, 1996; Brinkhuis and Zachariasse, 1988; Adatte et al., 2002a,b), the detrital increase is likely due to erosion of uplifted areas and/or influx from deltaic complexes to the south (Schnack and Luger, 1998; Schnack, 2000; Tantawy et al., 2001). A gradual increase in smectite during the early Danian (zones Pla–Plc) reflects a sea-level rise and/or increased seasonality.

8. Conclusions

1. Gebel Qreiya contains one of the most complete K/T boundary transitions in Egypt, as indicated by the presence of the characteristic K/T boundary red layer and Ir anomaly. However, there are frequent short hiatuses due to local tectonic activity and global sea-level changes, as evident by the short and incomplete planktic foraminiferal and calcareous nannofossil zones.

2. Planktic foraminiferal assemblages are generally impoverished, with species diversity about half of normal marine conditions and assemblages dominated by ecological generalists and opportunists.

3. Stable isotope analysis of the left and right coiling benthic foraminifer *Cibicidoides pseudoacutus* indicates no significant difference between right and left coiling species in either $\delta^{13}C$ or $\delta^{18}O$ values, suggesting that coiling ratio is not related to temperature or nutrient levels.

4. Stable isotope data indicate surface productivity was greatly decreased during zone CF3, creating an inverse surface-to-deep gradient, possibly because of the influence of deltaic complexes to the south exacerbated by local tectonic conditions and global sea-level regressions.

5. Normal environmental conditions were established during the latest Maastrichtian zone CF1 (upper *Micula prinsii* zone), when climate warmed and surface productivity increased, but surface productivity again decreased significantly at the end of the Maastrichtian.

6. During the early Danian, faunal and stable isotopic data indicate that similarly fluctuating high-stress conditions prevailed in the Eastern Desert as elsewhere in the marginal eastern Tethys, with normal conditions established in the lower part of zone Plc, or calcareous nannofossil zone NP1c. Mineralogical data indicate increased erosion and detrital influx due to local tectonic activity.

7. During the late Cretaceous to early Danian, high abundance of kaolinite suggests warm wet, tropical and subtropical conditions characterized by low seasonality contrasts, and predominantly chemical weathering (high kaolinite and smectite, very low mica and chlorite contents).

8. Observed hiatuses (e.g. CF3/CF1, CF1/P0, P0/Pla, P1a/P1b intervals) generally correspond to increases in chlorite and mica to the detriment of smectite and kaolinite, and suggest significant mechanical erosion of nearby uplifted areas and/or influx from deltaic complexes to the south. The coeval increase in smectite and chlorite observed near the top of the Maastrichtian may also indicate drier conditions (seasonality) in elevated areas, whereas dominance of kaolinite suggests more humid conditions with enhanced runoff prevailed in low-lying areas.

Acknowledgements

We are grateful to Wolfgang Stinnesbeck for field assistance and discussions, Zsolt Berner and Doris Stueben for Ir analysis of the K/T red clay, and Sigal Abramovich for faunal discussions and assistance in SEM illustrations. We thank the reviewers Peter Luger and W.J. Zachariasse for their suggestions and helpful comments. This study was sponsored by the U.S.–Egypt Science and Technology Joint Fund in cooperation with NSF and NRC under Project OTH2-008-001-98, NSF INT-9811030 (GK), and the Swiss National Fund No. 8220-028367 (TA).

References

Abdelmalik, W.M., Bassiouni, M.A., Obeid, F.L., 1978. Biostratigraphy of Upper Cretaceous lower Tertiary rocks from West central Sinai; 1, Planktic foraminifera. Ann. Mines Geol. 28, 181–215.

Abdel Razik, T.M., 1969. Stratigraphical studies on the phosphate deposits between River Nile and Red Sea (south latitude 27°N). Fac. Sci. Bull. Cairo Univ. 42, 299–324.

Abdel Razik, T.M., 1972. Comparative studies on the Upper Cretaceous-Early Paleogene sediments on the Red Sea coast, Nile Valley and Western Desert, Egypt. 6th Arab Petroleum Congress, Algeria, pp. 1–23.

Abramovich, S., Almogi, L.A., Benjamini, C., 1998. Decline of the Maastrichtian pelagic ecosystem based on planktic foraminifera assemblage change; implication for the terminal Cretaceous faunal crisis. Geology 26, 63–66.

Adatte, T., Rumley, G., 1989. Sedimentology and mineralogy of Valanginian and Hauterivian in the stratotypic region (Jura mountains, Switzerland). In: Wiedmann, J. (Ed.), Cretaceous of the Western Tethys. Proc. 3rd Int. Cretaceous Symp., Tübingen 1987. Scheizerbart'sche Verlagsbuchhandlung, Stuttgart, pp. 329–351.

Adatte, T., Stinnesbeck, W., Keller, G., 1996. Lithostratigraphic and mineralogic correlations of near K/T boundary clastic sediments in northeastern Mexico: Implications for origin and nature of deposition. Geol. Soc. Am. Spec. Paper 307, 211–226.

Adatte, T., Keller, G., Stinnesbeck, W., 2002. Late Cretaceous to Early Paleocene climate and sea-level fluctuations. Palaeogeogr. Palaeoclimatol. Palaeoecol. 178, 165–196.

Adatte, T., Keller, G., Burns, S., Stoykova, K.H., Ivanov, M.I., Vangelov, D., Kramer, U., Stueben, D., 2002. Paleoenvironment across the Cretaceous-Tertiary transition in eastern Bulgaria. Geol. Soc. Am. Spec. Paper 356, 231–252.

Almogi-Labin, A., Flexer, A., Honigstein, A., Rosenfeld, A., Rosenthal, E., 1990. Biostratigraphy and tectonically controlled sedimentation of the Maastrichtian in Israel and adjacent countries. Rev. Esp. Paleontol. 5, 41–52.

Apellaniz, E., Baceta, J.I., Benrnaola-Bilbao, G., Nunez-Betelu, K., Orue-Etxebarria, X., Payros, A., Pujalte, V., Robin, E., Rocchia, R., 1997. Analysis of uppermost Cretaceous-lowermost Tertiary hemipelagic successions in the Basque Country (western Pyrenees): evidence for a sudden extinction of more than half planktic foraminiferal species at the K/T boundary. Bull. Soc. Geol. France 168, 783–793.

Barrera, E., 1994. Global environmental changes preceding the Cretaceous-Tertiary boundary: Early-upper Maastrichtian transition. Geology 22, 877–880.

Barrera, B., Keller, G., 1994. Productivity across the Cretaceous/Teriary boundary in high latitudes. Geol. Soc. Am. Bull. 106, 1254–1266.

Barrera, E., Savin, S.M., Thomas, E., Jones, C.E., 1997. Evidence for thermohaline-circulation reversals controlled by sea-level change in the latest Cretaceous. Geology 25, 715–718.

Barthel, W.K., Herrmann-Degen, W., 1981. Late Cretaceous and Early Tertiary stratigraphy in the Great Sand Sea and its SE Margins (Farafra and Dakhla Oases, SW Desert Egypt). Mitt. Bayer. Staatssamml. Paläontol. Hist. Geol. 21, 141–182.

Baum, G.R., Vail, P.R., 1988. Sequence stratigraphic concepts applied to Paleogene outcrops in the Gulf and Atlantic basins. In: Wilgus, C.K., Hastings, B.S., Kendall, C.G., Posamentier, W.W., Ross, C., van Wagoner, J.C. (Eds.), Sea Level Changes: An Integrated Approach. Soc. Econ. Paleontologists and Mineralogists Spec. Publ. 42, pp. 309–328.

Berggren, W.A., Kent, D.V., Swisher, C.C., III, Aubry, M.-P., 1995. A revised Cenozoic geochronology and chronostratigraphy. In: Berggren, W., Kent, D.V., Aubry, M.-P., Hardenbol, J. (Eds.), Geochronology, Time Scales and Global Stratigraphic Correlation, Soc. Sed. Geol., Spec. Publ. 54, pp. 129–212.

Brinkhuis, H., Zachariasse, W.J., 1988. Dinoflagellate cysts, sea level changes and planktonic foraminifers across the Cretaceous-Tertiary boundary at El Haria, northwest Tunisia. Mar. Micropaleontol. 13, 153–191.

Canudo, J.I., Keller, G., Molina, E., 1991. Cretaceous/Tertiary boundary extinction pattern and faunal turnover at Agost and Caravaca, SE Spain. Mar. Micropaleontol. 17, 319–341.

Caron, M., 1985. Cretaceous planktic foraminifera. In: Bolli, H.M., Saunders, J.B., Perch-Nielsen, K. (Eds.), Planktic Stratigraphy. Cambridge University Press, Cambridge, pp. 17–86.

Chamley, H., 1989. Clay Sedimentology. Springer, Berlin, 623 pp.

Chamley, H., 1998. Clay mineral sedimentation in the Ocean. In: Paquet, H., Clauer, N. (Eds.), Soils and Sediments (Mineralogy and Geochemistry). Springer, Berlin, pp. 269–302.

Coccioni, R., Galeotti, S., 1998. What happened to small benthic foraminifera at the Cretaceous/Tertiary boundary? Bull. Soc. Geol. France 169, 271–279.

Deconinck, J.F., Chamley, H., 1995. Diversity of smectite origins in Late Cretaceous sediments; example of chalks from northern France. Clay Min. 30, 365–379.

Donovan, A.D., Baum, G.R., Blechschmidt, G.L., Loutit, T.S., Plum, C.E., Vail, P.R., 1988. Sequence stratigraphic setting of the Cretaceous/Tertiary boundary in central Alabama. In: Wilgus, C.K., Hastings, B.S., Kendall, C.G., Posamentier, W.W., Ross, C., van Wagoner, J.C. (Eds.), Sea Level Changes: An Integrated Approach. Soc. Econ. Paleontologists and Mineralogists Spec. Publ. 42, pp. 309–328.

Espitalié, J., Deroo, G., Marquis, F., 1986a. La pyrolyse Rock-Eval et ses applications, première partie. Rev. Inst. Fr. Pét. 40, 563–579.

Espitalié, J., Deroo, G., Marquis, F., 1986b. La pyrolyse Rock-Eval et ses applications, seconde partie. Rev. Inst. Fr. Pét. 40, 755–784.

Espitalié, J., Deroo, G., Marquis, F., 1986c. La pyrolyse Rock-Eval et ses applications, troisième partie. Rev. Inst. Fr. Pét. 41, 73–89.

Faris, M., 1984. The Cretaceous-Tertiary boundary in Central Egypt, (Duwi region, Nile Valley, Kharga and Dakhla oases). N. Jahrb. Geol. Paläontol. Abh. 7, 385–392.

Faris, M., 1995. Late Cretaceous and Paleocene calcareous nannofossil biostratigraphy at St. Paul section, Southern Galala Plateau, Egypt. Ann. Geol. Surv. Egypt 20, 527–538.

Faris, M., 1997. Biostratigraphy of calcareous nannofossils across the K/T boundary in Egypt. N. Jahrb. Geol. Paläontol. Abh. 5, 447–464.

Fourcade, E., Rocchia, R., Gardin, S., Bellier, J.-P., Debrabant, P., Masure, E., Robin, E., Pop, W.T., 1998. Age of the Guatemala breccias around the Cretaceous–Tertiary boundary: relationships with the asteroid impact on the Yucatan. Comptes Rendues de l'Academie Scientifique Paris, Sciences de la Terre et des planètes 327, 47–53.

Galeotti, S., Coccioni, R., 2002. Changes in coiling direction of Cibicidoides pseudoacutus across the Cretaceous/Tertiary boundary transition of Tunisia: paleoecological and biostratigraphic implications. Palaeogeogr. Palaeoceol. Palaeoclimatol. 178, 197–210.

Ganz, H.H., Luger, P., Schrank, E., Brooks, P., Fowler, M., 1990. Facial evolution of Late Cretaceous black shales from Southeast Egypt. In: Klitzsch, E., Schrank, E. (Eds.), Research in Sudan, Somalia, Egypt and Kenya; results of the special research project 'Geoscientific problems in arid and semiarid areas' (Sonderforshungsbereich 69); period 1987–1990. Berliner Geowissenschaftliche Abhandlungen, Reihe A: Geologie und Paläontologie 120(2), pp. 993–1010.

Ganz, H.H., Schrank, E., Brooks, P.W., Fowler, M.G., 1990. Facies evolution of Late Cretaceous black shales from Southeast Egypt. In: Huc, Y. (Ed.), Deposition of Organic Facies, Am. Assoc. Pet. Geol. Bull. 30, pp. 229–217.

Garrison, R.F., Glenn, C.R., Snavely, P.D., Mansour, S.E.A., 1979. Sedimentology and origin of Upper Cretaceous phosphorite deposits at Abu Tartur, Western Desert, Egypt. Ann. Geol. Surv. Egypt 9, 261–281.

Gaucher, G., 1981. Les Facteurs de la Pedogenèse. G. Lelotte, Dison, 730 pp.

Gibbs, R.J., 1977. Clay mineral segregation in the marine environment. J. Sed. Pet. 47, 237–243.

Glenn, R.C., 1990. Depositional sequences of the Duwi, Sibaiya and Phosphate Formations, Egypt: phosphogenesis and glauconitization in a late Cretaceous epeiric sea. In: Notholt, A.J.G., Jarvis, I. (Eds.), Phosphorite Research and Development, Geol. Soc. Spec. Publ. 52, pp. 205–222.

Hendriks, F., Luger, P., Biwitz, J., Kallenbach, H., 1987. Evolution of the depositional environments of SE Egypt during the Cretaceous and lower Tertiary. Berl. Geowiss. Abh. (A) 75, 49–82.

Hendriks, F., Luger, P., 1987. The Rakhiya Formation of the Gebel Qreiya area: evidence of Middle Campanian to early Maastrichtian synsedimentary tectonism. Berl. Geowiss. Abh. (A) 75, 83–89.

Hermina, M., 1990. The surroundings of Kharga, Dakhla and Farafra oases. In: Said, R. (Ed.), The Geology of Egypt. A.A. Balkema, Rotterdam, pp. 259–292.

Issawi, B., 1972. Review of Upper Cretaceous-Lower Tertiary stratigraphy in central and southern Egypt. Am. Assoc. Pet. Geol. Bull. 56, 1448–1463.

Jenkyns, H.C., 1990. Impact of Mesozoic anoxic events on shallow-water carbonate facies. AGU 1990 fall meeting, EOS Trans. Am. Geophys. Union 71(43).

Jiang, M.J., Gartner, S., 1986. Calcareous nannofossil succession across the Cretaceous/Tertiary boundary in east-central Texas. Micropaleontology 32, 232–255.

Kassab, A.S., Keheila, E.A., 1994. Paleocene biostratigraphy and sea level changes of the northern Eastern Desert of Egypt. Newsl. Stratigr. 31, 85–100.

Keller, G., 1993. The Cretaceous/Tertiary boundary transition in the Antarctic Ocean and its global implications. Mar. Micropaleontol. 21, 1–45.

Keller, G., 2002. High-stress late Maastrichtian planktic foraminiferal assemblages mimic early Danian in Central Egypt, Mar. Micropaleontol., in press.

Keller, G., Lindinger, M., 1989. Stable isotopes, TOC and CaCO3 records across the Cretaceous-Tertiary boundary at El Kef, Tunisia. Palaeogeogr. Palaeoclimatol. Palaeoecol. 73, 243–265.

Keller, G., Benjamini, C., 1991. Paleoenvironment of the eastern Tethys in the Early Paleocene. Palaios 6, 439–464.

Keller, G., Barrera, E., Schmitz, B., Matsson, E., 1993. Grad-

ual mass extinction, species survivorship, and long term environmental changes across the Cretaceous-Tertiary boundary in high latitudes. Geol. Soc. Am. Bull. 105, 979–997.
Keller, G., Adatte, T., Stinnesbeck, W., Stuben, D., Kramar, U., Berner, Z., Li, L., Perch-Nielsen, K., 1998. The Cretaceous-Tertiary transition in the shallow Saharan Platform of southern Tunisia. Geobios 30, 951–975.
Keller, G., Li, L., MacLeod, N., 1995. The Cretaceous/Tertiary boundary stratotype section at El Kef, Tunisia: How catastrophic was the mass extinction? Palaeogeogr. Palaeoclimatol. Palaeoecol. 119, 221–254.
Keller, G., Adatte, T., Stinnesbeck, W., Luciani, V., Karoui, N., Zaghbib-Turki, D., 2002. Paleobiogeography of the Cretaceous-Tertiary mass extinction in planktic foraminifera. Palaeogeogr. Palaeoclimatol. Palaeoecol. 178, 257–298.
Keller, G., Stinnesbeck, W., 1996. Sea level changes, clastic deposits, and megatsunamis across the Cretaceous-Tertiary boundary. In: MacLeod, N., Keller, G., (Eds.), The Cretaceous/Tertiary Boundary Mass Extinction: Biotic and Environmental Changes. W.W. Norton, New York, pp. 415–450.
Keller, G., Stinnesbeck, W., Lopez-Oliva, J.G., 1994. Age, deposition and biotic effects of the Cretaceous/Tertiary boundary event at Mimbral, NE Mexico. Palaios 9, 144–157.
Keller, G., Adatte, T., Stinnesbeck, W., Stueben, D., Berner, Z., 2001. Age, chemo- and biostratigraphy of Haiti spherule-rich deposits: a multi-event K-T scenario. Can. J. Earth Sci. 38, 197–227.
Klitzsch, E., Wycisk, P., 1987. Geology of the sedimentary basins of northern Sudan and bordering areas. Berl. Geowiss. Abh. (A) 75, 47–79.
Kübler, B. 1983. Dosage quantitatif des minéraux majeurs des roches sédimentaires par diffraction X. Cahier de l'Institut de Géologie de Neuchâtel, Série ADX, Vol. 1, 12 pp.
Kübler, B. 1987. Cristallinité de l'illite, méthodes normaisées de préparations, méthodes normalisées de mesures. Cahiers Institut de Géologie, Neuchâtel, Suisse, Série ADX, Vol. 1.
Kucera, M., Malmgren, B.A., 1998. Terminal Cretaceous warming event in the mid-latitude South Atlantic Ocean: evidence from poleward migration of Contusotruncana contusa (planktonic foraminifera) morphotypes. Palaeogeogr. Palaeoclimatol. Palaeoecol. 138, 1–15.
Li, L., Keller, G., 1998a. Maastrichtian climate, productivity and faunal turnovers in planktic foraminifera in South Atlantic DSDP Sites 525 and 21. Mar. Micropaleontol. 33, 55–86.
Li, L., Keller, G., 1998b. Maastrichtian diversification of planktic foraminifera at El Kef and Elles, Tunisia. Eclogae Geol. Helv. 91, 75–102.
Li, L., Keller, G., 1998c. Abrupt deep-sea warming at the end of the Cretaceous. Geology 26, 995–999.
Li, L., Keller, G., Stinnesbeck, W., 1999. The Late Campanian and Maastrichtian in northwestern Tunisia: Paleoenvironmental inferences from lithology, macrofauna and benthic foraminifara. Cret. Res. 20, 231–252.
Li, L., Keller, G., Adatte, T., Stinnesbeck, W., 2000. Late Cretaceous sea level changes in Tunisia: a multi-disciplinary approach. J. Geol. Soc. London 157, 447–458.
Luciani, V., 1997. Planktonic foraminiferal turnover across the Cretaceous-Tertiary boundary in the Vajont valley (Southern Alps, northern Italy). Cret. Res. 18, 799–821.
Luciani, V., 2002. High resolution planktonic foraminiferal analysis from the Cretaceous/Tertiary boundary at Ain Settara (Tunisia): Evidence for an extended mass extinction. Palaeogeogr. Palaeoclimatol. Palaeoecol. 178, 299–320.
Luger, P., 1988. Maastrichtian to Paleocene facies evolution and Cretaceous/Tertiary boundary in middle and southern Egypt. Rev. Esp. Micropaleontol. Numero Extraordinario, 83–90.
Luger, P.E., Beshtawy, M., Mai, J., 1989. Maastrichtian planktonic foraminiferal biozonation and K/T boundary in Central Egypt. Rev. Esp. Micropaleontol. 30, 37–49.
Luger, P., Groeschke, M., 1989. Late Cretaceous ammonites from the Wadi Qena area in the Egyptian Eastern Desert. Palaeontology 32, 355–407.
MacLeod, N., Keller, G., 1991. How complete are Cretaceous/Tertiary boundary sections? A chronostratigraphic estimate based on graphic correlation. Geol. Soc. Am. Bull. 103, 1439–1457.
Magaritz, M., Benjamini, C., Keller, G., Moshkovitz, S., 1992. Early diagenetic isotopic signal at the Cretaceous/Tertiary boundary, Israel. Palaeogeogr. Palaeoclimatol. Palaeoecol. 91, 291–304.
Martini, E., 1971. Standard Tertiary and Quaternary calcareous nannoplankton zonation. Proc. 2nd Planktonic Conference (Rome, 1970), pp. 739–785.
Nederbragt, A.J., 1991. Late Cretaceous biostratigraphy and development of Heterohelicidae (planktic foraminifera). Micropaleontology 37, 329–372.
Nederbragt, A., 1998. Quantitative biogeography of late Maastrichtian planktic foraminifera. Micropaleontology 44, 385–412.
Olsson, R.K., Hemleben, C., Berggren, W.A., Huber, B.T., 1999. Atlas of Paleocene Planktonic Foraminifera. Smithsonian Contribution to Paleobiology No. 85. Smithonian Institution Press, Washington, DC, 252 pp.
Olsson, R.K., Wright, J.D., Miller, K.G., 2001. Paleobiogeography of Pseudotextularia elegans during the latest Maastrichtian global warming event. J. Foram. Res. 31, 275–282.
Pearson, P.N., Ditchfield, P.W., Singano, J., Harcourt-Brown, K.G., Nicholas, C.J., Olsson, R.K., Shackleton, N.J., Hall, M.A., 2001. Warm tropical sea surface temperatures in the Late Cretaceous and Eocene epochs. Nature 413, 481–487.
Perch-Nielsen, K., 1981a. New Maastrichtian and Paleocene calcareous nannofossils from Africa, Denmark, the USA and the Atlantic, and some Paleocene lineages. Eclogae Geol. Helv. 73, 831–863.
Perch-Nielsen, K., 1981b. Les nannofossiles calcaires à la limite Crétcé-Tertiaire prés de El Kef, Tunisie. Cah. Micropaleontol. 3, 25–37.
Perch-Nielsen, K., 1985. Cennozoic calcareous nannofossils. In: Bolli, H.M., Saunders, J.B., Perch-Nielsen, K., (Eds.), Plankton Stratigraphy. Cambridge University Press, Cambridge, pp. 422–454.
Porrenga, D.H., 1966. Clay minerals in recent sediments of the

Niger delta. Clays Clay Min., 14th Nat. Conf. Pergamon, Oxford, pp. 211–233.

Robaszynski, F., Caron, M., Gonzalez Donoso, J.M., Wonders, A.A.H., the European Working Group on planktonic foraminifera, 1983–1984. Atlas of Late Cretaceous Globotruncanids. Rev. Micropaleontol. 26, 145–305.

Robert, C., Chamley, H., 1991. Development of early Eocene warm climates, as inferred from clay mineral variations in oceanic sediments. Glob. Planet. Change 3, 315–331.

Robert, C., Kennett, J.P., 1992. Paleocene and Eocene kaolinite distribution in the South Atlantic and Southern Oceaan: Antarctic climatic and paleoceanographic implications. Mar. Geol. 103, 99–110.

Said, R., 1962. The Geology of Egypt. Elsevier, Amsterdam, 377 pp.

Schnack, K., Luger, P., 1998. Facies and structural evolution during the Maastrichtian and Paleocene in the Kharga uplift area and adjacent areas (Western Desert, SW-Egypt). Zbl. Geol. Palaeontol. Teil I, pp. 311–351.

Schnack, K., 2000. Biostratigraphie und fazielle Entwicklung in dem Oberkreide und im Alttertiär im Bereich der Kharga-Schwelle, Westliche Wuste, SW Aegypten. Berichte aus dem Fachbereich Geowissenschaften der Universität Bremen No. 151, 142 pp.

Schrank, E., 1984. Organic-walled microfossils and sedimentary facies in Abu Tartur phosphates (Late Cretaceous, Egypt). Berl. Geowiss. Abh. (A) 50, 177–187.

Sestini, G., 1984. Tectonic and sedimentary history of the NE African margin (Egypt-Libya). In: Dixon, J.E., Robertson, A.H.F. (Eds.), The Geological Evolution of the Eastern Mediterranean, Geol. Soc. Spec. Publ. 17, pp. 161–175.

Shahin, A., 1992. Copntribution to the foraminiferal biostratigraphy and paleobathymetry of the late Cretaceous and early Tertiary in the western central Sinai, Egypt. Rev. Micropal. 35, 157–175.

Sissingh, W., 1977. Biostratigraphy of Cretaceous calcareous nannoplankton. Geol. Mijnb. 56, 37–65.

Smith, A.G., Smith, D.G., Funnel, B.M., 1994. Atlas of Mesozoic and Cenozoic Coastlines. Cambridge University Press, 164 pp.

Soliman, M., Habid, M., Ahmed Ezzat, A., 1986. Sedimentologic and tectonic evolution of the Upper Cretaceous-lower Tertiary succession at Wadi Qena. Egypt. Sed. Geol. 46, 111–113.

Stinnesbeck, W., Keller, G., de la Cruz, J., de Leon, C., MacLeod, N., Whittaker, J.E., 1997. The Cretaceous–Tertiary transition in Guatemala: limestone breccia deposits from the South Peten basin. Geol. Rundsch. 86, 686–709.

Stott, L.D., Kennett, J.P., 1990. The paleoceanographic and climatic signature of the Cretaceous–Paleogene boundary in the Antarctic: Stable isotopic results of ODP Leg 113. Proc. ODP, Sci. Results 113, 829–848.

Strougo, A., Haggag, M., Luterbacher, H., 1992. The basal Paleocene 'Globigerina' eugubina Zone in the Eastern Desert (St. Paul's Monastery, South Galala), Egypt. N. Jahrb. Geol. Palaeontol. Mon.heft. 1992, 97–101.

Stueben, D., Kramar, U., Berner, Z., Stinnesbeck, W., Keller, G., Adatte, T., 2002. Trace elements and stable isotopes in foraminifera of the Elles II K/T profile: Indications for sea level fluctuations and primary productivity. Palaeogeogr. Palaeoclimatol. Palaeoecol. 178, 321–349.

Tantawy, A.A. 1998. Stratigraphical and paleontological studies on some Paleocene-Eocene successions in Egypt. Ph.D. Thesis, Aswan Faculty of Science, South Valley University, Egypt, 273 pp.

Tantawy, A.A., Keller, G., Adatte, T., Stinnesbeck, W., Kassab, A., Schulte, P., 2001. Maastrichtian to Paleocene (Dakhla Formation) depositional environment of the Western Desert in Egypt: sedimentology, mineralogy and integrated micro- and macrofossil biostratigraphies. Cret. Res. 22, 795–827.

Tantawy, A.A., in press. Calcareous nannofossil biostratigraphy and paleoecology of the Cretaceous-Tertiary transition in Central Eastern Desert, Egypt. Mar. Micropaleontol.

Weaver, C.E., 1989. Clays, Muds and Shales, Development in Sedimentology, Vol. 44. Elsevier, Amsterdam, 819 pp.

Zachos, J.C., Arthus, M.A., Dean, W.E., 1989. Geochemical evidence for suppression of pelagic productivity at the Cretaceous/Tertiary boundary. Nature 337, 41–64.